学 位 論 文

<< Solidification Processes of Ultramafic Cumulates in the Mikabu Belt, Central Japan >>

（みかぶ帯超苦鉄質集積岩の固結過程）

平成４年１２月博士（理学）　申請

東京大学大学院理学系研究科
地質学専攻
小澤　大成

①

Solidification Processes of Ultramafic Cumulates in the Mikabu Belt, Central Japan

Hiroaki OZAWA

Geological Institute
University of Tokyo

December, 1992

Abstract

Geological and petrological study was done in order to understand the nature of the ultramafic cumulates in the Mikabu belt. Solidification processes of ultramafic cumulates are discussed.

Representative geological feature of ultramafic complexes of the Mikabu belt can be observed in the Toba ultramafic complex. It is divided into three units. Unit I is composed of olivine cumulate and olivine clinopyroxene cumulate. Unit II is a sill complex of hornblende-rich rocks and overlies Unit I. Unit III is composed of hornblende-rich rocks and occurs as dikes intruding into Unit I. Unit I is characterized by the alternation of olivine cumulate and olivine clinopyroxene cumulate. The layering mostly strikes northwest to southeast and dips to east. This trend is similar to that of foliation and sills of Unit II. Olivine cumulate in Unit I is characterized by orthocumulate texture. The primary magma for the Toba complex can be estimated from the chemical composition of the dike from Unit III. It can coexist with mantle olivine and its MgO content is 14.4wt.%.

An unequilibrated olivine orthocumulate in the Mikkabi complex is described to understand nature of interstitial liquid crystallization. Olivine has zonal structure characterized by decrease of Fo and NiO contents which cannot be explained by fractional crystallization model. Chemical composition of spinel enclosed in olivine correlates to the distance to the rim of host olivine. TiO_2 and YFe of spinel increases as distance to rim decreases. Spinel chemistry also correlates to enclosed minerals and spinel enclosed in postcumulus phases is relatively rich in TiO_2 and YFe. Clinopyroxene has chemical zoning and the rim of clinopyroxene has higher TiO_2 and Na_2O and lower XMg. XMg of

clinopyroxene and other postcumulus phases are not so low as expected from incompatible elements enrichment. These lines of evidence suggest that the Fe/Mg ratio of interstitial liquid of this olivine cumulate is buffered by olivine while incompatible element is enriched by postcumulus crystallization.

Wide chemical variation of spinel even in one thin section in Unit I of the Toba complex suggests abundant influence of interstitial liquid crystallization. Although olivine is now completely homogenized, gentle decrease of NiO content(0.34 to 0.25wt.%) comparable to that of Fo content(88 to 81) supports trapped liquid crystallization. High TiO_2 and Na_2O contents of interstitial clinopyroxene can also be explained by trapped liquid fractionation.

Macrorhythmic unit of the olivine cumulate in the Toba complex is characterized by upward decrease of postcumulus phases modal content and upward increase of incompatible elements in spinel and clinopyroxene. Chemical composition of olivine usually does not change significantly. This layering is a direct evidence of boundary layer fractionation. Fractionated interstitial liquid buffered by olivine migrates from the bottom and chemical composition of spinel and clinopyroxene are affected.

Olivine cumulate of the Shimoina complex is characterized adcumulus texture and planar fabric of interstitial spinel. Chemical composition of olivine and spinel may not be significantly affected by interstitial liquid crystallization. Cyclic unit can be defined by the chemical composition of the olivine and spinel. The melt column height required to form each units by fractional crystallization is estimated to be a few hundreds meters thick. Secondary reducing of porosity in the Shimoina complex may not have been occurred because time scale for compaction may be longer than the cooling

time scale. In situ crystallization with low porosity is preferable for the Shimoina adcumulate. The crystal mush with low porosity is now deformed. Fabric and Al-Cr chemical zoning of spinel and well attained texture equilibrium of olivine suggest that the mechanism of the deformation is solution and precipitation. The chemical variation and texture of ultramafic cumulate in the Toba complex and the Shimoina complex is distinct, however, the size of the chamber is same order of magnitude. The difference is probably caused by the production rate of the magma.

Contents

List of Figures

List of Tables

List of Plates

Plate5-1 Photographs of the thin sections of the macrorhythmic unit of olivine cumulate in the columnar section from the Toba ultramafic complex. A: Base of a macrorhythmic unit. B: Top of a macrorhythmic unit. Note abundant interstitial phases in A and texture equilibrium in B. The width of the photograph is c. a. 7mm.

Plate6-1 A: Olivine cumulate of Unit I in the Shimoina complex. This thin section is vertical to the foliation. S304-2. Note well attained texture equilibrium. Base part of the columnar section. B: Olivine clinopyroxene cumulate of Unit I. S232. The width of the photograph is c. a. 7mm.

Plate6-2 A: Olivine clinopyroxene plagioclase cumulate in Unit I. This thin section is vertical to the foliation. S310-3. The width of the photograph is c. a. 7mm. B: Vein of clinopyroxene in olivine cumulate. S68. The width of the photograph is c. a. 3.5mm.

I. Introduction

1. Purpose of this study

There are two important views of cumulate. One is that cumulate has a direct evidence for magma chamber processes and the other is that cumulate has important information for melt segregation process because cumulate is solidified product from crystal and liquid mixture.

Recently crystallization of crystal mush is thought to be significant for evolution of volcanic rocks(Langmuir, 1989; Nielsen and DeLong, 1992). Chemical composition of volcanic rock is not direct evidence of fractional crystallization. In volcanic rocks, we can only observe integrated melt composition although systematic correlation of chemical composition can give some constraints.

Melt extraction from mixture of melt and solid plays an important role in melt segregation in the mantle(McKenzie, 1984) and lower crust. Cumulate can give some constraint for evolution of crystal mush.

Mineral chemical composition and texture of cumulate have direct information for crystallization processes because we can spatially and sequentially investigate magma chamber. But the mineral chemical composition of cumulate is possibly modified by the reaction with interstitial liquid(e.g. Barnes, 1986) and subsolidus reequilibration(e.g. Ozawa, 1984). Some elements which have large diffusion coefficients can be changed easily. Trend and degree of modification should be discussed to evaluate effects for magma evolution.

The purpose of this study is to discuss solidification processes of ultramafic cumulates. Solidification processes include crystallization and reaction of interstitial liquid, migration of

interstitial liquid and subsolidus reequilibration. After we understand these processes, we can use information of cumulates.

Ultramafic cumulates in the Mikabu belt is target for this study. In Chapter II, geology of the Toba complex will be presented for representative geological feature of the ultramafic complexes of the Mikabu belt. In Chapter III, an unequilibrated orthocumulate from the Mikkabi complex will be described to understand the chemical evolution trend of the interstitial liquid. In Chapter IV, subsolidus reequilibration of ultramafic cumulates from the Toba complex will be discussed. In Chapter V, origin of macrorhythmic units in the Toba complex will be considered. In Chapter VI, petrological feature of the Shimoina complex will be described and origin of adcumulates in it will be discussed.

2. Cumulate terminology

A Cumulate is defined as an igneous rock characterized by a framework of touching crystals that evidently were concentrated through fractional crystallization of their parental magmatic liquid(Irvine, 1982). Cumulates are usually classified as orthocumulates, mesocumulates or adcumulates based on the amount of postcumulus materials, which appear to have crystallized from interstitial liquid(Irvine, 1982). However it is difficult to determine the amount of postcumulus materials because they include overgrowth on cumulus material. In this paper, cumulates are classified into two types by the amount of interstitial minerals. Adcumulates have 0-7% of interstitial minerals, typically have mutual interference boundaries. Orthocumulates have more than 7% of interstitial minerals. Cumulus grains in orthocumulates typically exhibit their euhedral shape.

In order to describe the layering, following terms are introduced. Cyclic units are repeated successions of layers in which the rock sequence can be identified with the fractional crystallization path(Irvine, 1982). Macrorhythmic units are rhythmically repeated successions of relatively thick(1-10m) modaly distinctive layers, which is not clear whether the composition variations are directly related to fractional crystallization path(Irvine, 1982).

3. Analytical method

Mineral chemistry

The chemical composition of minerals were determined by electron microprobe X-ray analyzers JEOL JCXA-733 of Ocean Research Institute and JCMA-733 MkII of Geological Institute, both of the University of Tokyo. The accelerating voltage was 15kv, the specimen currents were 1.2×10^{-8} A and the counting time was 30s. The correction procedure is according to Bence and Albee(1968) and the correction factors are taken from Nakamura and Kushiro(1970). The ferric iron content of spinel was calculated from the charge balance considerations. Total iron is assumed to be equal to Fe^{2+} except for spinel. For the precise determination of Ni and Mn content in Olivine, the following conditions were applied; accelerating voltage = 25kv, the specimen current = 2.0×10^{-8} A, the counting time = 200s, for the both of Ni and Mn. The correction procedures were based on ZAF method. Cation ratios are abbreviated as follows: $XMg=Mg/(Mg+Fe^{2+})$; $YCr=Cr/(Cr+Al+Fe^{3+})$; $YFe=Fe^{3+}/(Cr+Al+Fe^{3+})$.

Bulk rock chemistry

The samples were crushed into coarse powder in a WC mill and ground into fine powder in a agate ball mill. For the analysis, 0.4g of dried rock powder was used. Sample-flux(lithium tetra borate) ratio was 1:10. The mixture of sample and flux was made into glass beed. Analyses were carried out with the Rigaku System 3080ES XRF of the Earthquake Research Institute, University of Tokyo. JB-1 and/or JB-2(rock reference samples from Geological Survey of Japan) were repeatedly analyzed in order to confirm the analyses. All Fe are analyzed as ferrous(FeO*).

II Geology of the Toba ultramafic complex: a case study of the Mikabu belt

1. Introduction

The Mikabu belt is an accreted oceanic crust discontinuously extended up to 900km between the Sambagawa belt and the Chichibu belt. The Mikabu belt consists of basaltic volcanic rocks, mafic-ultramafic complex and chert. Lower limit of the age of accretion is thought to be Jurassic according to the age determined by radioralia(Iwasaki et al., 1984).

The tectonic setting of igneous activity was believed to be oceanic island origin(Nakamura, 1986; Isozaki et al, 1990). The crystallization sequence in volcanic rocks from olivine to clinopyroxene followed by plagioclase(Nakamura, 1971) is quite different from that of MORB(e.g. Shido et al., 1971). The depleted lead isotope (Hamelin et al., 1984) suggests that the tectonic setting of the Mikabu belt is different from island arc. Estimated primary magma for the Mikabu belt is rich in MgO(e.g. Nakamura, 1971; Yoshida et al, 1984) and different from that of MORB.

Some ultramafic complexes of the Mikabu belt have been investigated by Tazaki(1966), Nakamura(1971), Inomata(1978) and Makimoto(1978). According to their studies, especially detailed petrological and geological study of Nakamura(1971), the general stratigraphic sequence of the mafic-ultramafic complex is proposed as follows. The stratigraphically lowest cumulate consists of dunite and wehrlite with occurrence of minor olivine clinopyroxene gabbro. Sheet complex composed of hornblende-rich rocks overlies mafic-ultramafic cumulates and this is overlain by basaltic volcanic

rocks. No definite residual peridotite has been reported from the Mikabu belt.

The detailed structure of layering and cumulate classification of ultramafic rocks have not been clearly presented yet. In this chapter, I clarify the petrological feature of the ultramafic cumulate at the Toba ultramafic complex. I also present a candidate of primary melt of the Toba complex.

2. Geological setting

The Toba ultramafic complex is one of ultramafic masses of the Mikabu belt. It is located on the eastern coast of Kii peninsula, 34°30'N and 136°50'E(Fig.2-1). The first detailed petrological study of the Toba ultramafic complex was done by Nakamura(1971).

In the Toba area, several lenticular masses of ultramafic rock are distributed in weakly metamorphosed sedimentary rocks and basic volcanic rocks. The Chichibu belt is distributed in the southern part. The Chichibu belt is in fault contact with the Sambagawa belt in this district. Sedimentary rocks of this district are mainly chert laminite(Yoshida, 1981) with small amount of volcanic mudstone and rare sandstone. The general bedding trend of the sedimentary rocks is EW strike and mostly south dip. The basic volcanic rocks are pillow lava, massive lava and pyroclastics. The assemblage of the phenocryst are olivine + spinel, olivine + clinopyroxene + spinel and clinopyroxene. The ultramafic complex is in fault contact with the host rock. The fault strikes EW and dips south on northern side.

Detailed investigation was made on the Sugashima island because of the good exposure of the whole succession of mafic and ultramafic rocks.

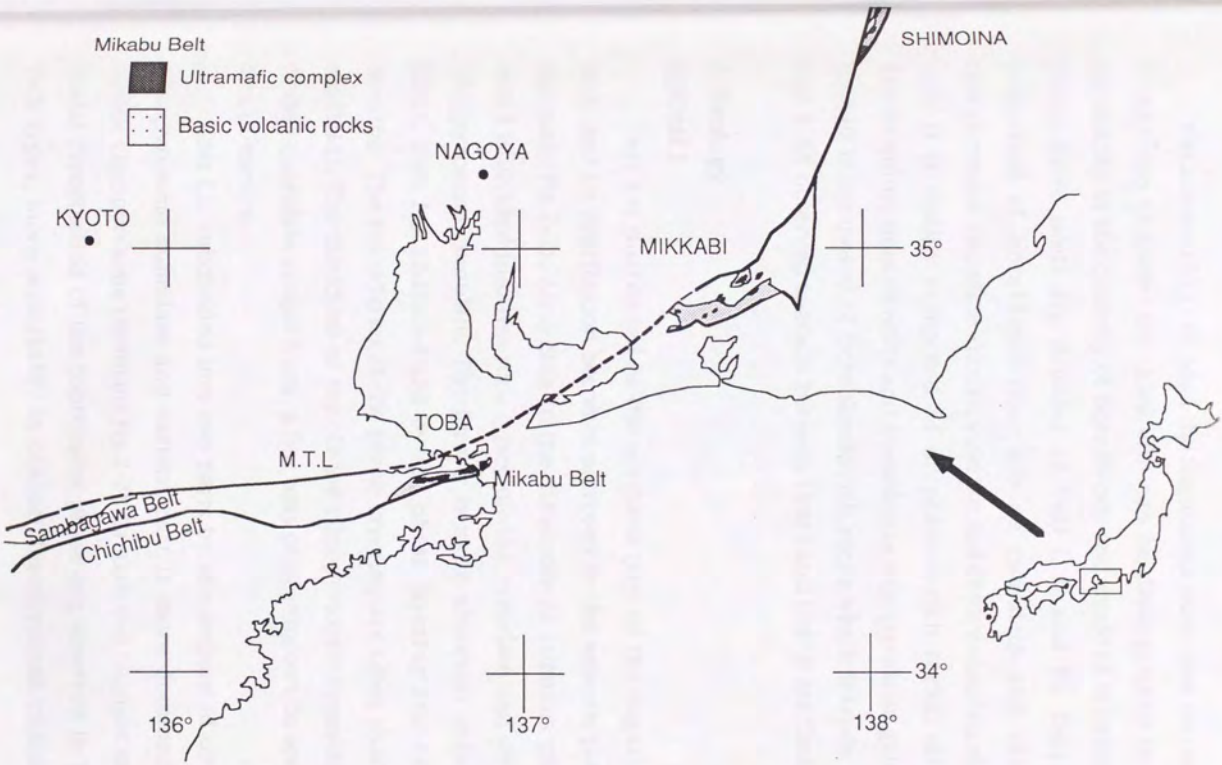

Fig.2-1 Index map of the ultramafic masses of the Mikabu belt, central Japan.

Nakamura(1971) divided the Sugashima mass into two units. In addition to them the third unit can be distinguished by the peculiarity in the quantity of hornblende and mode of occurrence: These three units are denoted as Unit I, II and III. Unit I is composed of hornblende-poor olivine cumulate and olivine clinopyroxene cumulate: dunite, wehrlite and clinopyroxene gabbro. Unit II is mainly composed of hornblende-rich rocks, olivine hornblendite, hornblendite and hornblende clinopyroxene gabbro. Unit III is composed of hornblende-rich rocks which intrude into Unit I. All observed contacts between Unit I and Unit II are faults.

3. Geology

(1)Unit I

Unit I is distributed in the northern part of the Sugashima mass and its distribution becomes narrower in the western part of the mass(Fig.2-2). According to the difference of cumulus phase, Unit I is divided into two rock types: olivine cumulate and olivine clinopyroxene cumulate. The former is more abundant than the latter. Unit I is characterized by the phase layering and modal layering. The boundaries of the phase layering are often sharp in the fields. The thickness of the olivine clinopyroxene cumulate in olivine cumulate ranges from a few tens of centimeters to several tens of meters.

Unit I is subdivided into two parts by the amount of olivine clinopyroxene cumulate and eastern part is more dominant in olivine clinopyroxene cumulate(Fig.2-2). Gradational changes in the modal composition of the constituent phase are observed in both rock types, more remarkably in olivine clinopyroxene cumulate.

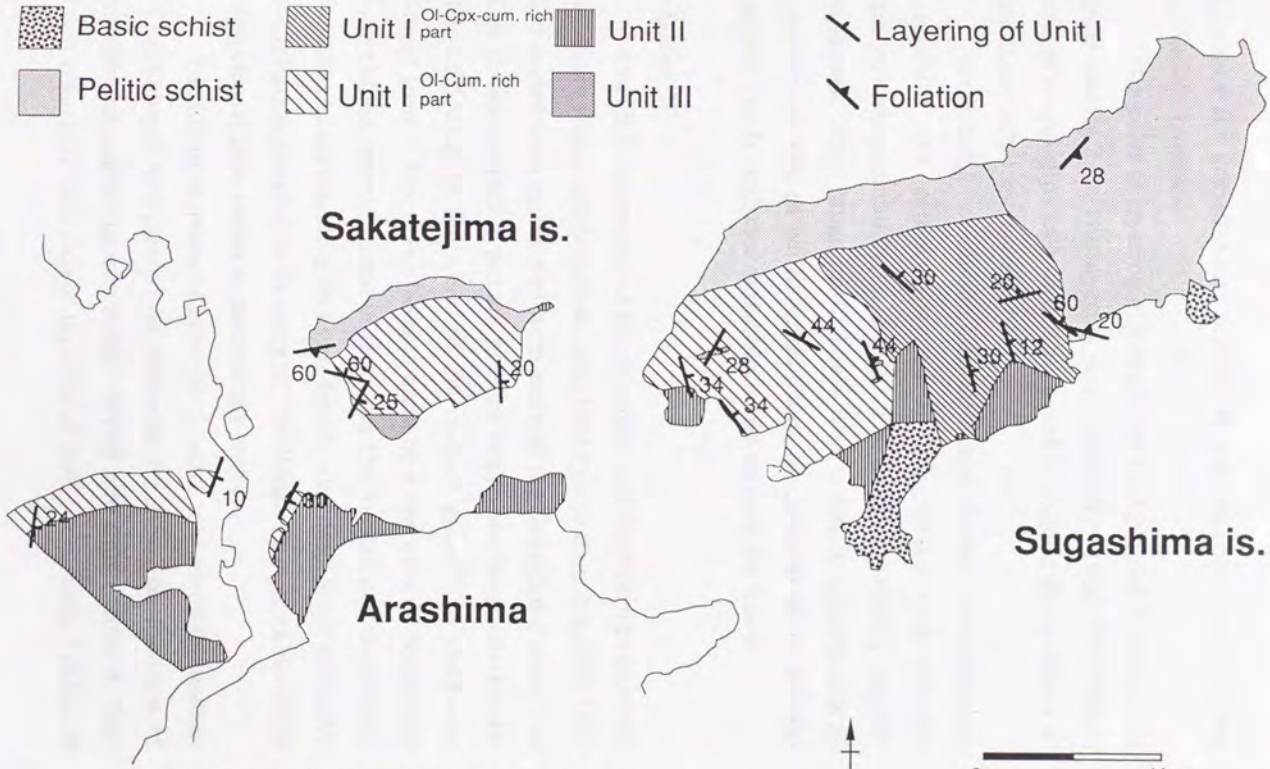

Fig.2-2 Geological map of the Toba ultramafic complex (Sugashima mass)

Evidence for gravitational settling is not observed in the Toba ultramafic complex.

The poles of layering planes of Unit I are plotted in equal area diagrams(Fig.2-3). The layering plane generally strikes NNW-SSE to NNE-SSW and dips eastward. This trend is oblique to the trend of the major lithologic boundary.

Platy blocks of olivine cumulate and olivine clinopyroxene cumulate are often observed in plagioclase-rich olivine clinopyroxene cumulate(Plate 2-1B). The blocks are locally angular in shapes. They range in thickness from a few to several tens of centimeters and in width several tens of centimeters to several meters. The boundaries of the block and its host are sharp.

(2) Unit II

Unit II is composed of hornblendite and hornblende gabbros which are richer in hornblende than Unit I(more than 40vol.%). Unit II is distributed in the southern part of the Sugashima mass. In Unit II, various rock types are present, which are interpreted to be sills according to the trend of the contact plane. The thickness ranges from a few tens of centimeters to a few meters. Some sills have chilled margin. Some of them cut the foliation of the others. Xenoliths of surrounding rocks are locally observed. Some sills have the foliation parallel to its margin. The lineation of hornblende is most remarkably shown in hornblende gabbro.

The foliation, plane of intrusive contact, and mineral lineation of hornblende are plotted on stereonet(Fig.2-3). The foliation of hornblende gabbro mostly strikes NW-SE and dips eastward. This trend coincides with that of layering of Unit I and contact plane of

A. Layering of Unit I

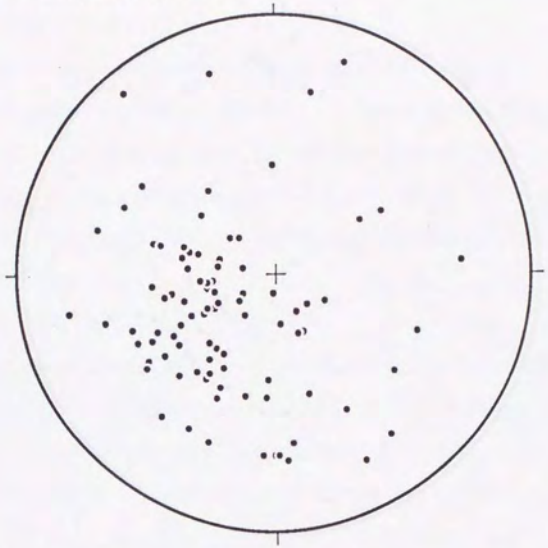

B. Dyke of Unit III

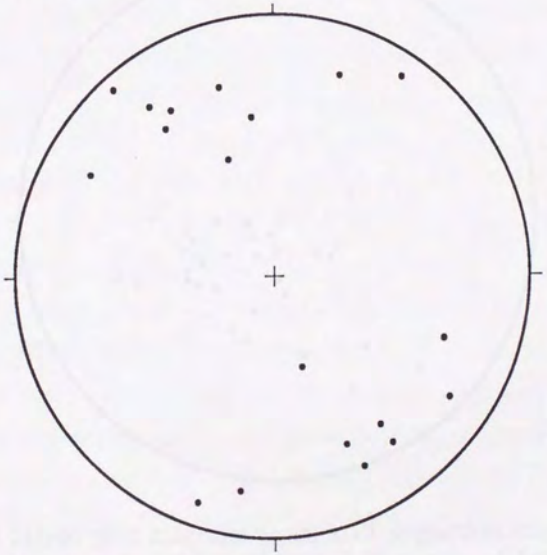

Fig.2-3 Stereo plot diagram: equal area projection. A: Pole of layering of Unit I B: Pole of intrusive contacts of Unit III.

C. Host of Unit II

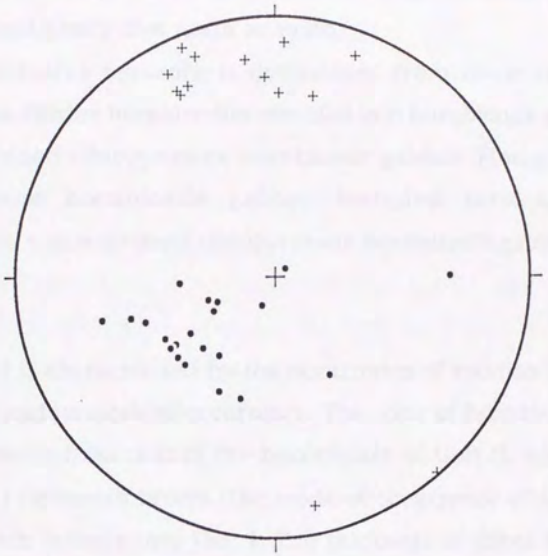

D. Intrusives of Unit II

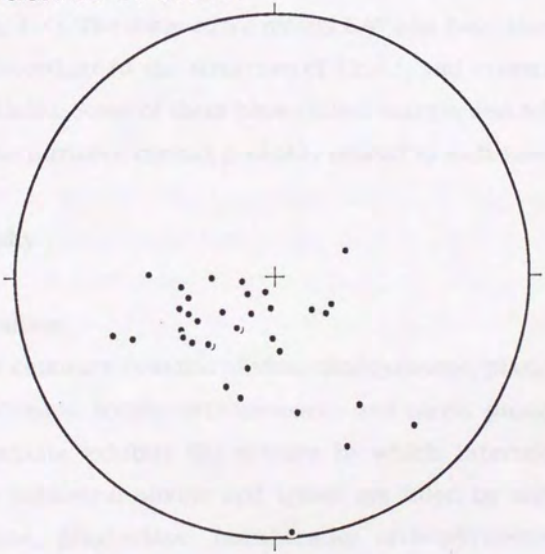

Fig.2-3 Stereo plot diagram: equal area projection.(Continued) C: Host hornblende gabbro of Unit II. dot: pole of foliation plus: lineation of hornblende D: Pole of intrusive contacts of Unit II.

the intrusion. The lineation of hornblende in hornblende gabbro strikes N-S and gently dips north or south.

The intrusive sequence is determined from those contact relationships. Olivine hornblendite intruded into hornblende gabbro and fine grained clinopyroxene hornblende gabbro. Fine grained clinopyroxene hornblende gabbro intruded into olivine hornblendite, coarse grained clinopyroxene hornblende gabbro.

(3)Unit III

Unit III is characterized by the occurrence of reddish brown hornblende and its mode of occurrence. The color of hornblende is clearly different from that of the hornblende of Unit II, which is pale brown to greenish brown. The mode of occurrence of Unit III is dikes which intrude into Unit I. The thickness of dikes ranges from 20 to 100cm. The poles of the intrusive contacts are plotted on stereonet(Fig.2-3). The dikes strike mostly E-W and have steep dip. They are discordant to the structure of Unit I, and crosscut the layering of Unit I. Some of them have chilled margin and foliation parallel to the intrusive contact probably related to melt flow.

4. Petrography

(1) Unit I

Olivine cumulate

Olivine cumulate contains olivine, clinopyroxene, plagioclase, spinel, hornblende, locally orthopyroxene and rarely phlogopite. Olivine cumulate exhibits the texture in which interstices of euhedral to subhedral olivine and spinel are filled by anhedral clinopyroxene, plagioclase, hornblende, orthopyroxene and phlogopite(Plate 2-2A). They are dunite or wehrlite. Representative

modal compositions are shown in Table 2-1. The locality of the sample is shown in Fig.2-4.

Olivine is euhedral to subhedral and sometimes equigranular in olivine-rich rock. The grain size of olivine ranges generally from 2 to 7mm. Olivine sometimes contains inclusions of magnetite forming network pattern of naturally decorated olivine(Zauch and Green, 1977). Some olivine grains show wavy extinction. Olivine is partly altered to serpentine and chlorite. Spinel is usually almost opaque and euhedral to subhedral and locally irregular. Spinel is enclosed by olivine, clinopyroxene, plagioclase, hornblende or occurs along grain boundaries. Irregular shape spinel occurs along grain boundaries. The grain size of spinel is up to 2mm. Spinel is partly altered to magnetite. Clinopyroxene is pale green and anhedral. Poikilitic clinopyroxene including olivine is often observed. Exsolution lamellae of spinel is always found in clinopyroxene. Clear marginal parts free of spinel lamellae are observed in clinopyroxene. The margin has different extinction angle from the core. Hornblende partly replaces some clinopyroxene grains. Clinopyroxene is partly altered to tremolite. Plagioclase is anhedral and completely altered to aggregate of grossular and pumpellyite except for one grain included in olivine(Plate 2-3). Hornblende is anhedral and shows reddish brown to pale brown pleochroism. Poikilitic hornblende including olivine is sometimes present. Some veins of pale brown hornblende, up to 1mm thick, cut olivine cumulate.

Olivine clinopyroxene cumulate

Olivine clinopyroxene cumulate contains olivine, clinopyroxene, plagioclase, hornblende, spinel and rarely

Sample No.	Rock Type	Ol mode	Cpx mode	Pl mode	Sp mode	Hb mode	Phg mode	Opx mode	Avg. Fo
T011110	Oc	81.2	7.9	9.1	1.2	0.4			84.7
T31253	Occ	63.5	16.5	18.9	1.3	0.0			83.5
T05138	Oc	95.6	0.8		3.5				85.7
T29253	Oc	79.5	17.9	0.7	1.8	0.0			82.5
T041110	Oc	77.3	21.8	0.3	0.5				82.5
T28253	Oc	85.6	7.3	4.5	2.3	0.1			83.9
T061110	Oc	91.6	4.7	0.6	1.2	1.8			82.4
T071110	Oc	18.8	43.1	37.7	0.0	0.2			
T05158	Oc	78.0	15.2	2.4	2.9	1.4		0.0	84.7
T04158	Occ	32.3	33.5	32.1	0.2	1.7		0.0	83.2
T02158	Oc	85.9	7.1	4.3	1.6	0.9		0.0	84.9
T141510	Occ	64.6	18.6	15.1	1.7	0.0			83.4
T221410	Oc	78.4	18.5	0.6	1.5	0.6			84.0
T110810	Oc	72.8	17.7	0.6	1.2	1.8			80.7
T020410	Oc	86.1	4.2	4.6	2.3	2.1	0.4	0.1	87.9

Table2-1 Representative modal compositions and Fo content of Unit I: Oc; olivine cumulate, Occ; olivine clinopyroxene cumulate.

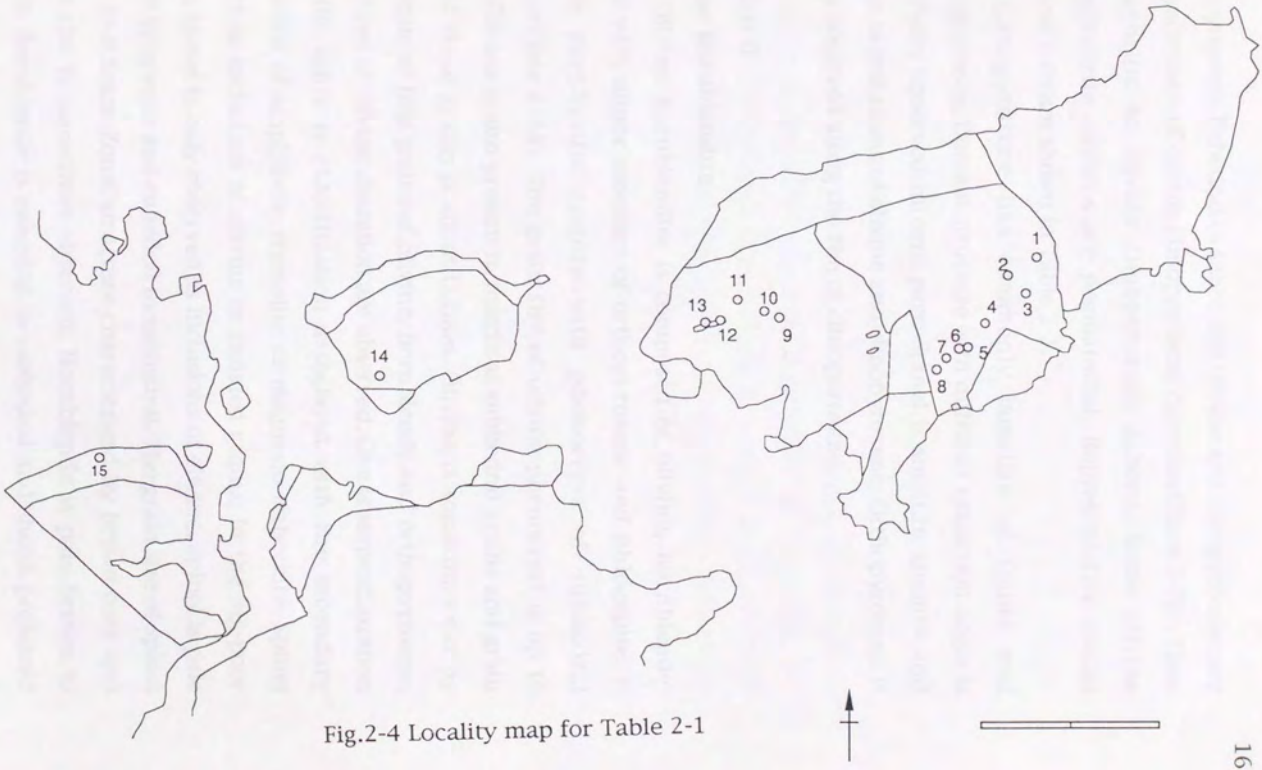

Fig.2-4 Locality map for Table 2-1

orthopyroxene. Euhedral to subhedral olivine and clinopyroxene are a characteristic of olivine clinopyroxene cumulate(Plate 2-2B). They are wehrlite to olivine clinopyroxene gabbro. Some olivine clinopyroxene gabbros are pegmatoidal. Representative modal compositions are shown in Table 2-1.

Clinopyroxene has commonly lamellae of spinel and orthopyroxene. Domain structure with different extinction angle is sometimes observed in core part. Spinel is small in amount and occurs as inclusions of olivine and clinopyroxene. Orthopyroxene is rarely observed along the rim of clinopyroxene.

(2) Unit II

Olivine hornblendite

Olivine hornblendite is composed of olivine, hornblende, spinel with minor amounts of orthopyroxene and phlogopite. It shows porphyritic texture with phenocryst of subhedral olivine(Plate 2-4A). The grain size of olivine phenocryst is up to 1cm. Olivine is also present in matrix as subhedral grains and grain size of these grains is about 0.1mm. Olivine is sometimes cut by aggregate of fine grains of olivine, hornblende and orthopyroxene. Two types of olivine alteration are observed. One is serpentinization and the other is chloritization associated with the secondary formation of amphibole, tremolite or magnesio riebeckite. Spinel occurs as inclusions of olivine or isolated grains. In the Mg-poor rocks, spinel is only observed as inclusions of olivine. Spinel is pale brown to opaque and euhedral to subhedral. The grain size of spinel is up to 0.5mm. Zonal structure characterized by brown core and green rim is sometimes observed. Hornblende is pale brown to brown. Hornblende is euhedral to subhedral and shows preferred

shape orientation. The grain size of hornblende is about 0.1mm. It is sometimes altered to tremolite. Orthopyroxene is equidimensional, found in groundmass. It is often altered to chlorite. Phlogopite is rarely found in groundmass and is reddish brown.

Hornblende gabbro

Hornblende gabbro is the most dominant rock type in Unit II. It is composed of brown hornblende, plagioclase, ilmenite and rarely apatite. Hornblende gabbro has remarkable lineation of hornblende and weak foliation. The hornblende is subhedral. The grain size of hornblende is up to 0.5mm. Some of hornblende are altered to tremolite. Plagioclase is completely altered to grossular.

Clinopyroxene hornblende gabbro

Clinopyroxene hornblende gabbro is composed of clinopyroxene, hornblende, plagioclase and ilmenite. On the basis of grain size and texture, the clinopyroxene hornblende gabbro is classified into two types. Coarse-grained gabbro is characterized by porphyritic texture with clinopyroxene as a phenocryst. Clinopyroxene is usually poikilitic and includes euhedral laths of plagioclase. The exsolution lamellae of opaque mineral is commonly observed in clinopyroxene. Usually clinopyroxene is partly replaced by green hornblende. Clinopyroxene is sometimes completely altered to hornblende aggregate. The grain size of clinopyroxene is about 2.5mm. In fine-grained gabbro, clinopyroxene is subhedral to anhedral and exsolution lamellae of opaque mineral is not observed. The grain size of clinopyroxene is 0.1mm. Occasionally anhedral coarse grained clinopyroxene is present, which is partly

replaced by hornblende and has exsolution lamellae of opaque mineral.

(3) Unit III

The dikes of Unit III is classified into two rock types: porphyritic rocks and gabbroic rocks. Gradational change from one type to the other is not observed.

Porphyritic rocks

The phenocryst assemblage of the porphyritic rocks is olivine and spinel. Phenocryst of olivine is commonly found in the center of the dike. Olivine is euhedral and measures up to 5mm. The grain size of olivine increases from margin to center of the dike. These features suggest flow differentiation of olivine phenocrysts in these dikes. Olivine has sometimes magnetite inclusions, which are aligned as a network. Spinel is euhedral, occurs in the olivine or as an isolated grain and measures up to 2mm. The groundmass of porphyritic rocks is composed of hornblende, plagioclase and clinopyroxene. Hornblende is equidimensional and reddish brown. Although plagioclase is completely altered to grossular, the original lath shape is still preserved. Clinopyroxene is partly replaced by hornblende. Sometimes aphyric rocks occur, which are composed of fine hornblende grains and small amount of plagioclase(Plate2-4B).

Gabbroic rocks

The constituent minerals of the gabbroic rocks are hornblende, clinopyroxene, plagioclase, olivine and ilmenite. Olivine is anhedral and measures up to 0.5mm. Clinopyroxene is anhedral and measures up to 0.5mm. Hornblende is anhedral and measures

up to 0.3mm. Sometimes pegmatoidal texture is observed and the grain size of the hornblende is up to 2cm. Gabbroic rocks in Unit III are distinguished from those of Unit II because olivine coexists with clinopyroxene in Unit III whereas does not in Unit II.

5. Bulk rock chemistry

Bulk chemical composition of 15 specimens for Unit II and Unit III were determined by XRF(Table 2-2). The MgO content of Unit II decreases in the following order; olivine hornblendite, plagioclase hornblendite and clinopyroxene hornblende gabbro. In Fig.2-5, MgO content versus TiO_2, CaO, NiO and Al_2O_3 contents are plotted with the data of Nakamura(1971). The data points for Unit II and Unit III are mostly overlapping with those of volcanic rocks. The TiO_2 content increases as MgO content decreases.

6. Discussion

Primary magma of the Toba ultramafic complex

It is difficult to know the melt composition directly from gabbros because accumulation of crystals may occur in these coarse-grained rocks. However hornblendite (T071911, Table2-2, Plate2-4B) in Unit III is thought to preserve liquid composition because it consists of very fine hornblende and plagioclase up to 0.1mm with small amount of olivine phenocryst altered to chlorite. Such texture suggests that it represents rapidly cooled aphyric melt containing abundant water.

It is probable that fractionation of olivine only occurred in this rock because of its high MgO content(14.4wt.%, Table2-2) and phenocryst assemblage. According to the method of Takahashi et al.(1987), primary magma composition is estimated by addition of

	Sample No.	SiO2	TiO2	Al2O3	FeO*	MnO	MgO	CaO	Na2O	K2O	P2O5	FeO*/MgO	Na+K
Unit II	T062611b	43.50	0.58	6.80	11.02	0.16	31.53	5.46	0.88	0.04	0.03	0.35	0.92
Unit II	T032711a'	45.21	1.00	9.90	11.42	0.17	21.87	8.52	1.69	0.18	0.05	0.52	1.86
Unit II	T05211a	50.01	0.55	7.15	10.52	0.09	18.92	11.42	1.23	0.08	0.03	0.56	1.31
Unit II	T072611ac	46.30	1.03	10.86	11.24	0.15	17.39	11.01	1.81	0.13	0.06	0.65	1.95
Unit II	T111911a	47.14	1.21	13.31	11.50	0.16	12.25	12.16	2.10	0.08	0.07	0.94	2.18
Unit II	T062611a	44.25	1.68	13.73	13.88	0.21	10.04	14.63	1.39	0.09	0.11	1.38	1.47
Unit III	T071911	44.46	1.38	13.45	10.86	0.11	14.25	12.65	2.57	0.20	0.09	0.76	2.77
Unit III	T01297	43.61	2.01	14.10	13.84	0.19	9.98	15.18	0.90	0.04	0.15	1.39	0.94
Unit III	T07118	44.78	1.28	12.28	12.14	0.17	13.05	13.30	2.84	0.09	0.07	0.93	2.93
Unit III	T012211	44.40	1.31	12.02	12.59	0.18	14.26	12.97	1.83	0.36	0.08	0.88	2.19
Unit III	T111405b1	44.42	1.19	11.99	12.58	0.17	12.61	14.36	2.23	0.39	0.07	1.00	2.62
Unit III	T02263b	43.77	1.23	11.53	13.66	0.19	14.61	12.40	2.18	0.36	0.07	0.94	2.54
Unit III	T081911a	43.42	1.28	11.48	12.82	0.19	16.11	12.51	1.90	0.23	0.08	0.80	2.13
Unit III	T120810	46.94	1.13	13.05	11.77	0.16	12.49	12.51	1.93	0.02	0.00	0.94	1.95
Unit III	T010911	46.41	1.01	11.74	11.86	0.18	15.24	11.16	2.23	0.14	0.05	0.78	2.36

Table2-2 Bulk chemical compositions of Unit II and Unit III.

	Sample No.	Rb	Sr	Ba	Y	Zr	V	Cr	Ni	Cu	Zn	Nb	La	Ce	Sc	Th
Unit II	T062611b	0.0	33.5	0.0	8.9	28.7	148.1	2200.4	1848.7	17.1	74.0	0.8	1.8	0.0		0.0
Unit II	T032711a'	2.0	53.6	5.2	13.9	49.3	236.6	1759.0	1081.8	7.7	118.9	2.6	7.2	10.9		0.1
Unit II	T05211a	1.0	21.7	0.0	8.0	27.6	133.6	2690.0	643.1	117.0	56.9	0.8	7.9	22.3		0.8
Unit II	T072611ac	0.0	68.5	0.0	14.7	52.5	279.0	1294.5	755.6	113.3	71.7	1.3	9.7	22.3		0.6
Unit II	T111911a	0.0	175.1	0.0	18.0	56.6	335.9	934.8	348.4	99.5	70.4	2.9	4.5	30.3		1.9
Unit II	T062611a	0.0	250.5	0.0	26.0	75.2	468.8	412.4	185.4	213.5	87.1	3.6	9.1	16.6		1.5
Unit III	T071911	0.0	150.5	1.5	20.5	69.9	353.3	973.9	453.3	23.3	41.5	2.2	0.0	26.7		2.2
Unit III	T01297	0.0	146.8	1.4	25.6	755.3	501.0	195.7	127.3	208.5	89.9	2.2	0.0	20.1		0.0
Unit III	T07118	0.0	3781.5	224.9	16.4	0.6	320.9	913.6	458.5	143.6	79.8	1.2	0.0	19.4		0.5
Unit III	T012211	11.7	231.0	0.0	26.7	105.8	650.4	1717.0	788.5	231.5	122.6	2.9	9.5	24.1	54.8	0.3
Unit III	T111405b1	7.5	1211.8	181.6	17.4	43.8	348.3	905.4	356.5	158.9	80.1	1.7	0.0	15.0	32.2	0.0
Unit III	T02263b	8.4	760.4	130.0	17.3	48.6	330.3	962.9	429.9	163.0	86.1	2.0	3.6	13.4	31.3	0.0
Unit III	T081911a	6.3	57.8	7.3	17.4	64.6	304.3	1965.8	589.1	157.7	71.6	2.2	9.6	26.3	32.9	1.7
Unit III	T120810	0.0	159.9	0.0	12.4	9.9	393.1	916.0	398.6	288.6	55.8	0.7	11.8	20.3	37.8	0.0
Unit III	T010911	2.5	82.3	2.7	17.2	49.0	317.3	1310.6	552.0	148.0	92.6	0.7	12.9	11.6	33.2	1.2

Table2-2 Bulk chemical compositions of Unit II and Unit III.(Continued)

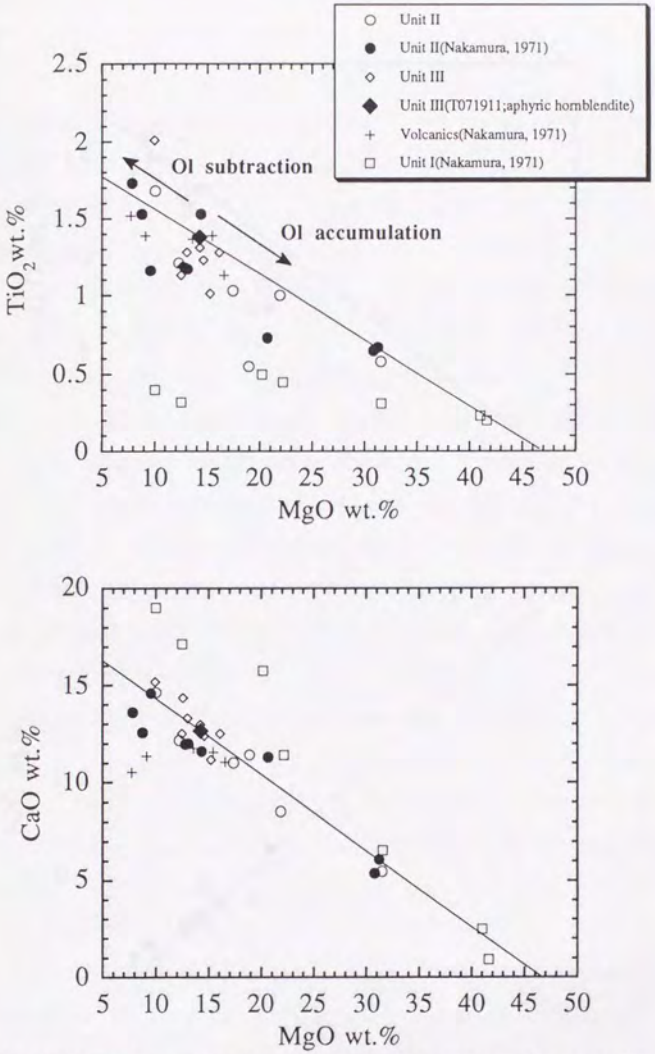

Fig.2-5 Bulk rock compositions of the Toba ultramafic complex. For The data of Nakamura(1971) is also plotted: open circle; Unit II filled circle; Unit II(Nakamura, 1971) open diamond; Unit III filled diamond; aphyric hornblendite(T071911) of Unit III plus; volcanics(Nakamura, 1971), open square; Unit I(Nakamura, 1971) Calculated accumulation-subtraction trend of the olivine for aphyric hornblendite(T071911) is shown. The chemical composition of olivine is calculated according to Takahashi et al.(1987).

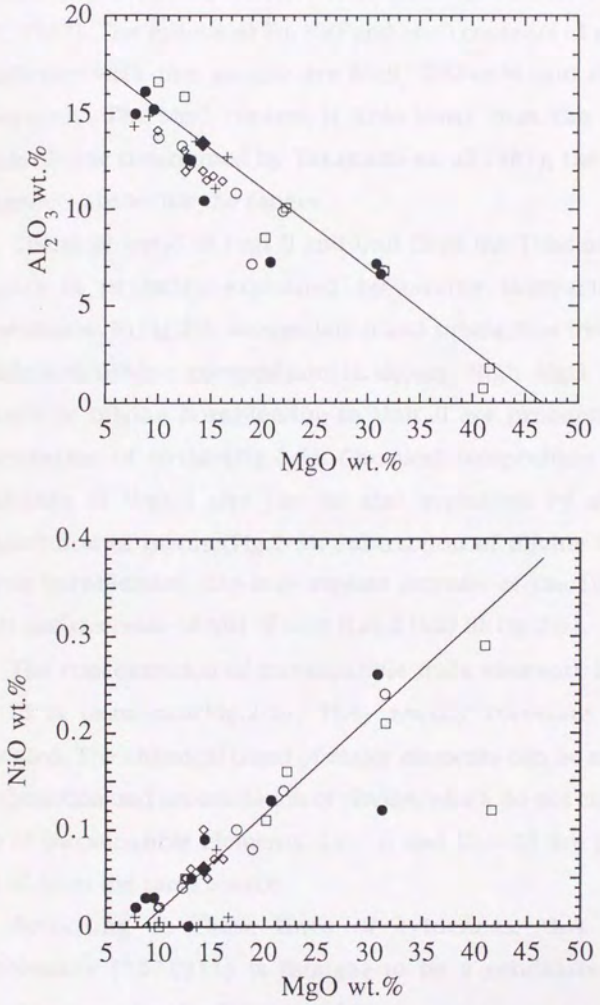

Fig.2-5 Bulk rock compositions of the Toba ultramafic complex(Continued). Calculated accumulation-subtraction trend is also shown.

equilibrium olivine to this hornblendite. The calculation suggests that this rock can be equilibrium with mantle peridotite(Takahashi et al., 1987). The estimated Fo, NiO and MnO contents of olivine in equilibrium with this sample are 86.9, 0.38wt.% and 0.09wt.%, respectively. The MnO content is little lower than the range of mantle olivine determined by Takahashi et. al(1987), the NiO and Fo contents are within the ranges.

Chemical trend of Unit II and Unit III of the Toba ultramafic complex is probably explained by olivine subtraction and accumulation. In Fig.2-5, accumulation and subtraction trend of the equilibrium olivine composition is shown. High MgO and NiO contents of olivine hornblendite in Unit II are probably due to accumulation of olivine(Fig.2-5). Chemical composition of some peridotites of Unit I also can be also explained by abundant accumulation of olivine(Fig.2-5). Subtraction of olivine from the aphyric hornblendite also may explain increase of the TiO_2, CaO, Al_2O_3 and decrease of NiO of Unit II and Unit III(Fig.2-5).

The concentration of incompatible trace elements in Unit II and III is examined(Fig.2-6). They mostly correlate linearly correlated. The chemical trend of major elements can be explained by subtraction and accumulation of olivine, which do not change the ratio of incompatible elements. Unit II and Unit III are probably derived from the same source.

According to these lines of evidences, this aphyric hornblendite (T071911) is thought to be a candidate for the primary magma for the Toba complex.

The MgO content of T071911 is 14.4wt.%. Nakamura(1971) discussed primary liquid of the Toba ultramafic complex by SI value and he concluded that primary magma is picrite basaltic

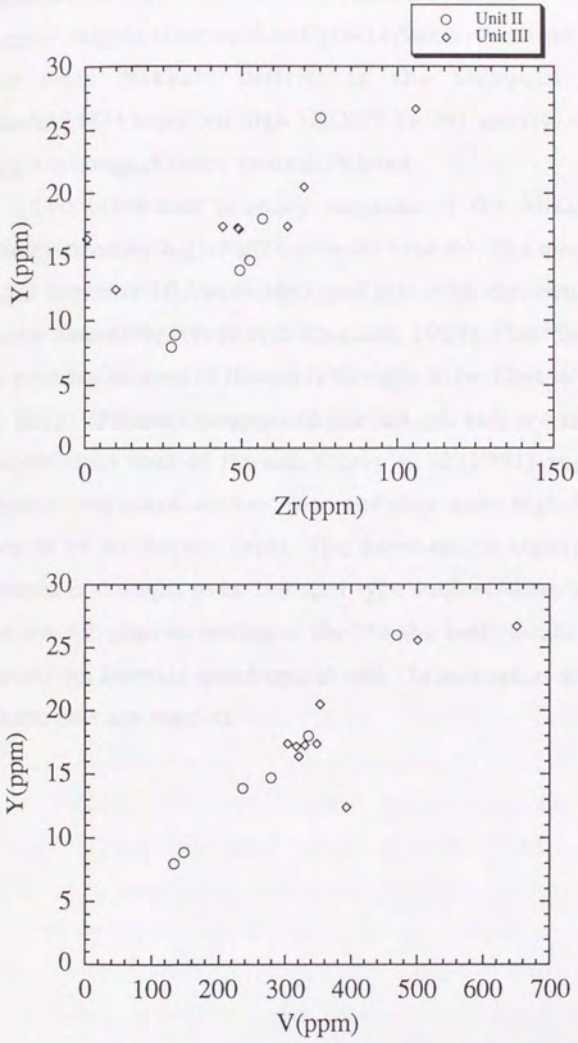

Fig.2-6 Trace element diagram for Unit II and Unit III. One sample with extremely high Zr content(T01297) is not included for Zr-Y diagram.

composition(MgO=13.1wt.%). Yoshida et al.(1984) presented a primary magma composition(MgO=14.5wt.%) from the study of the dike from Mikkabi district in the Shizuoka prefecture. Takeda(1984) reported high MgO(19.8wt.%) aphyric volcanic rock from Toyonaga district, central Shikoku.

The estimated primary magmas of the Mikabu belt are characterized by high MgO content(>13wt.%). The most magnesian MORB contains 10.6wt.% MgO and this rock can equilibrate with mantle assemblage(Fujii and Bougault, 1983). The MgO content of the primary magma of Hawaii is thought to be 12wt.%(Feigenson et al., 1983). Primary magmas of the Mikabu belt are richer in MgO content than that of Hawaii. Storey et al.(1991) suggested that primary magma of oceanic plateaus may have high MgO content because of its thicker crust. The geochemical signature of most plateaus is thought to be hot-spot type source(Storey et al., 1991). The oceanic-plateau setting of the Mikabu belt(Isozaki et al., 1990) is possible. Further geochemical and chronological studies of the Mikabu belt are needed.

III. Petrology of an unequilibrated olivine orthocumulate from the Mikkabi complex, central Japan.

1. Introduction

Recently, solidification of crystal mush is thought to be important because of its ability to make a different chemical trend of magma compositions from simple fractional crystallization, and it is called in situ fractionation (Langmuir, 1989) or boundary layer fractionation (Nielsen and DeLong, 1992). Boundary layer fractionation is characterized by ability to enrich incompatible elements with relatively small change in concentrations of compatible elements. Although some calculation was done to understand behaviors of the chemical trend(Langmuir, 1989; Nielsen and DeLong, 1992), cumulates may give information to understand the mechanism of this process. I believe that mineralogy of ultramafic cumulates is important information to visualize magma chamber processes.

It is recognized very difficult to discuss boundary layer crystallization by the chemical composition of the cumulate because usually cooling rate of ultramafic cumulate is too slow to preserve original chemical zonation in each grain. Observed chemical variations in cumulates are resulted from integration of magmatic and subsolidus processes. This is partly because a mineral to be used for discussion is olivine(e.g. Irvine, 1980). The cation diffusivities coefficient of olivine are large enough for homogenization during subsolidus cooling process(e.g. Morioka, 1981).

Chromian spinel is very useful mineral to understand the boundary layer processes. Because some elements, such as Ti and

Fe^{3+}, which are incompatible with olivine can be highly concentrated to Chromian spinel. In some cumulates, chemical variations even in the same thin section can be observed and is probably from evolution of interstitial liquid(Roeder and Campbell, 1985). Even in these samples, XMg values of spinel cannot preserve original value because subsolidus Fe-Mg exchange rate between spinel and enclosing minerals is usually rapid. Sample from lava lake is very useful to discuss chemical trend of spinel(Scowen et al., 1991), but relation between postcumulus phases and spinel cannot be directly observed because cooling rate is too high for interstitial liquid to form poikilitic cumulate texture.

The sample of olivine cumulate from the Mikkabi ultramafic complex is completely crystallized with poikilitic orthocumulate texture and preserves chemical zoning even in olivine. It is very important to know the chemical variation of this sample because the chemical trend in orthocumulate can be observed not only in chromian spinel but also in olivine and other postcumulus minerals. Cumulate are usually products from crystal mush, which has higher ratio of crystal to liquid than erupted magmas. We can discuss detailed boundary crystallization process only after we directly understand the magmatic chemical trend in cumulate.

2. Geological setting

The Mikkabi ultramafic complex is located to the north of the Hamana lake, Shizuoka Prefecture, central Japan(Fig.2-1). It is one of ultramafic complexes of the Mikabu belt. The Mikkabi ultramafic complex is composed of several masses with diameters from several hundred meters to a few kilometers. The ultramafic masses are concordantly distributed in host basic volcanic rocks(Inomata,

1978). The ultramafic masses are in fault contact with host rocks. Clastic rocks derived from ultramafic rocks are observed and interpretated as subaqueous gliding deposits(Saito et al., 1979).

The complex is composed of dunite, wherlite and clinopyroxene gabbro. The range of Fo content of olivine is from 83 to 80.5(Inomata and Tazaki, 1974; Inomata, 1979). An content of plagioclase is 84 and Fo content of coexisting olivine is 83(Inomata, 1979). Yoshida et al.(1984) estimated primary magma composition from the geochemical study of a picrite dike in the Kannonyama mass. MgO content of estimated primary magma is 14.5 wt.%.

According to detailed petrographic observation under microscope, the Mikkabi ultramafic complex can be divided into three units similar to the Toba ultramafic complex. Unit I, II, and III are composed of ultramafic cumulate(olivine cumulate, olivine clinopyroxene cumulate and clinopyroxene gabbro), hornblende-rich dike complex, dikes which intruded into Unit I, respectively. The orthocumulate sample described here belongs to Unit I. It should be mentioned that this heterogeneous rock is different from those homogenized ultramafic cumulates which usually observed in the Mikkabi complex.

3. Petrography

The sample is composed of olivine, spinel, clinopyroxene, plagioclase, orthopyroxene, hornblende, phlogopite and ilmenite(Plate 3-1). Modal compositions of this sample are 62.5% of olivine, 1.6% of spinel, 18.9% of clinopyroxene, 14.3% of plagioclase, 0.5% of orthopyroxene, 2% of hornblende with trace amount of phlogopite and ilmenite. It has orthocumulate texture. Olivine is euhedral to subhedral and the grain size of olivine is up to 3mm.

Olivine is partly altered to serpentine. Spinel is euhedral to subhedral and the grain size is up to 0.2mm. Spinel is enclosed by olivine, clinopyroxene, plagioclase or occurs along grain boundaries of these minerals. Clinopyroxene is pale green, anhedral and shows poikilitic texture. The grain size of clinopyroxene is up to 1cm. Fine platy opaque exsolution, which is commonly observed from the other ultramafic complexes of the Mikabu belt, cannot be observed. Plagioclase is anhedral and occurs in interstices of olivine. It is completely altered to grossular. Orthopyroxene is anhedral and occurs interstitially to olivine grains. It is partly altered to chlorite. Hornblende is anhedral and occurs in interstitial space of olivine. The color of hornblende is reddish brown. Ilmenite occurs as inclusions of hornblende. No spinel inclusions are found in hornblende. Phlogopite is anhedral and occurs in interstitial space of olivine. The color of phlogopite is reddish brown.

Since olivine and spinel are euhedral and included by other minerals, olivine and spinel are cumulus phases of this sample. Postcumulus phases are clinopyroxene, plagioclase, orthopyroxene, hornblende, phlogopite and ilmenite.

4. Mineral chemistry

Olivine

Olivine has chemical heterogeneity which is shown in Fig.3-1 and Plate3-2. Olivine typically has core composition of 90 in Fo content, 0.39wt.% in NiO, 0.15wt.% in MnO, and 0.3wt.% in CaO; and the rim composition of 79, 0.26wt.%, 0.32wt.%, 0.2wt.%, respectively.

Line analyses of selected olivine were performed and is shown in Fig.3-2. Fo content is fairly constant in the core and

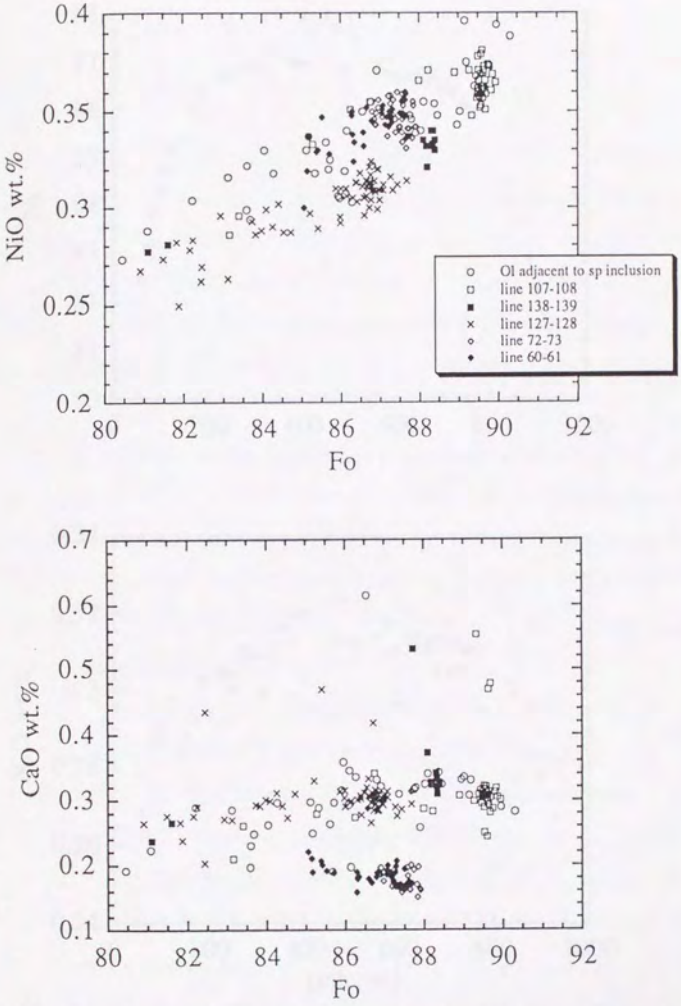

Fig.3-1 Chemical variation of olivine in the olivine orthocumulate from the Mikkabi complex. Analyses were performed with acceleration voltage 25KV.

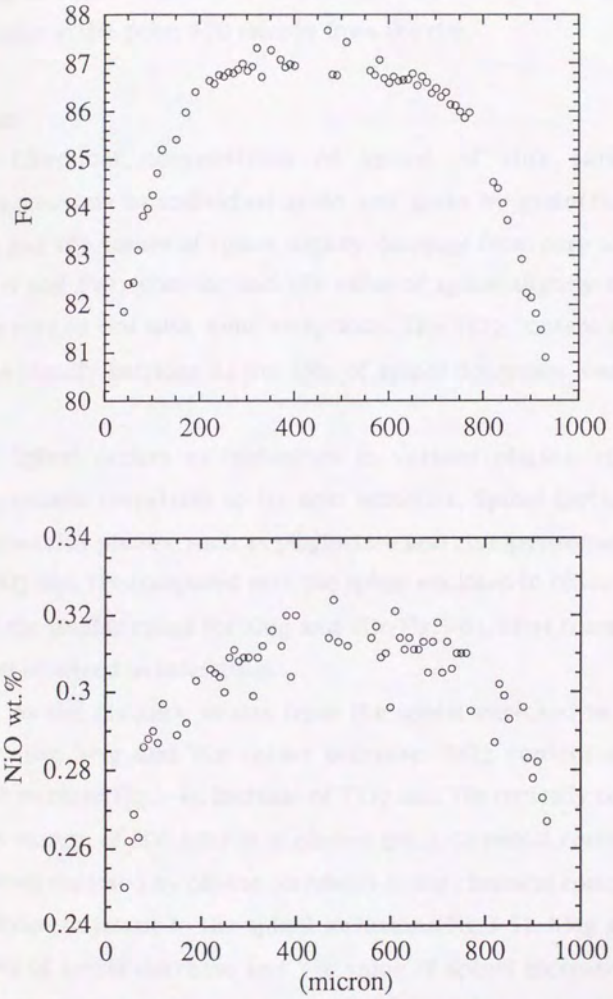

Fig.3-2 Line analyses of selected olivine grain. Scan step is 10 micron. The analyses was performed by EPMA with acceleration voltage 25kv.

begins to decrease outward about 200 micron from the rim. The shape of zonal structure is convex upward. NiO content begins to decrease at the point 120 micron from the rim.

Spinel

Chemical composition of spinel of this sample is heterogeneous in individual grain and grain by grain(Plate3-2). XMg and YCr values of spinel slightly decrease from core to rim of spinel and TiO_2 content and YFe value of spinel slightly increase from core to rim with some exceptions. The TiO_2 content and YFe value rapidly increase as the XMg of spinel decreases lower than 0.4.

Spinel occurs as inclusions in various phases, chemical composition correlates to its host minerals. Spinel included by postcumulus phases, such as plagioclase and clinopyroxene, is rich in TiO_2 and YFe compared with the spinel enclosed in olivine which is in the similar range for XMg and YCr(Fig.3-3). Most fractionated spinel occurred in interstitial.

As the distance to rim from the spinel enclosed in olivine decreases, XMg and YCr values decrease, TiO_2 content and YFe value increase(Fig.3-4). Increase of TiO_2 and YFe typically occurs in outer margin of 200 micron of olivine grain. Chemical composition of spinel enclosed by olivine correlates to the chemical composition of olivine adjacent to the spinel inclusions(Fig.3-5). XMg and YCr values of spinel decrease and YFe value of spinel increases as Fo content of olivine decreases. As Fo content decreases, the TiO_2 content slightly increases till Fo content of adjacent olivine achieves 85. Below Fo content is 85, the TiO_2 content shows large scatter

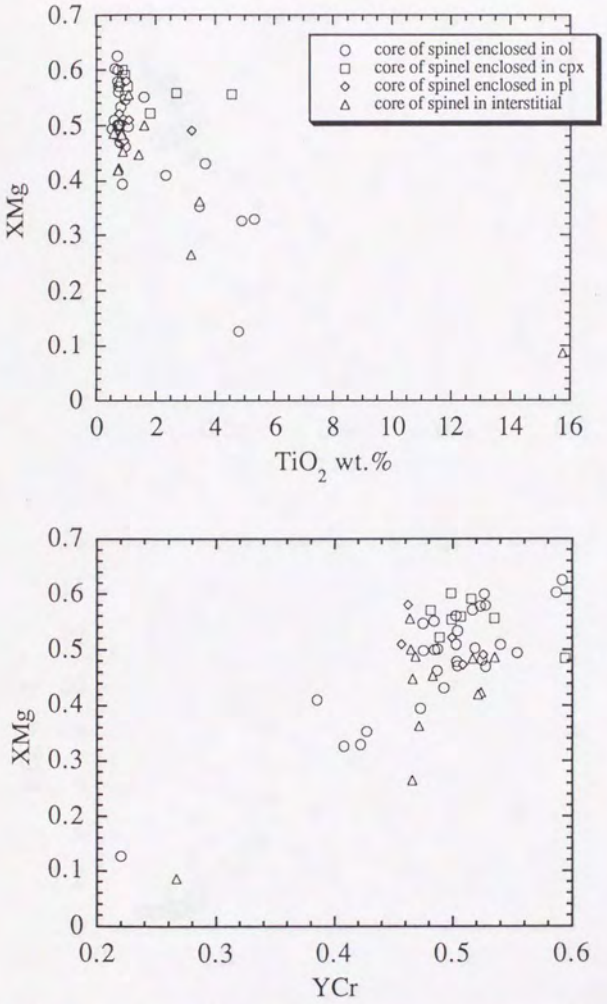

Fig.3-3 Chemical variation of core of spinel: open circle; inclusion in olivine, open square; inclusion in clinopyroxene, open diamond; inclusion in plagioclase, open triangle; interstitial.

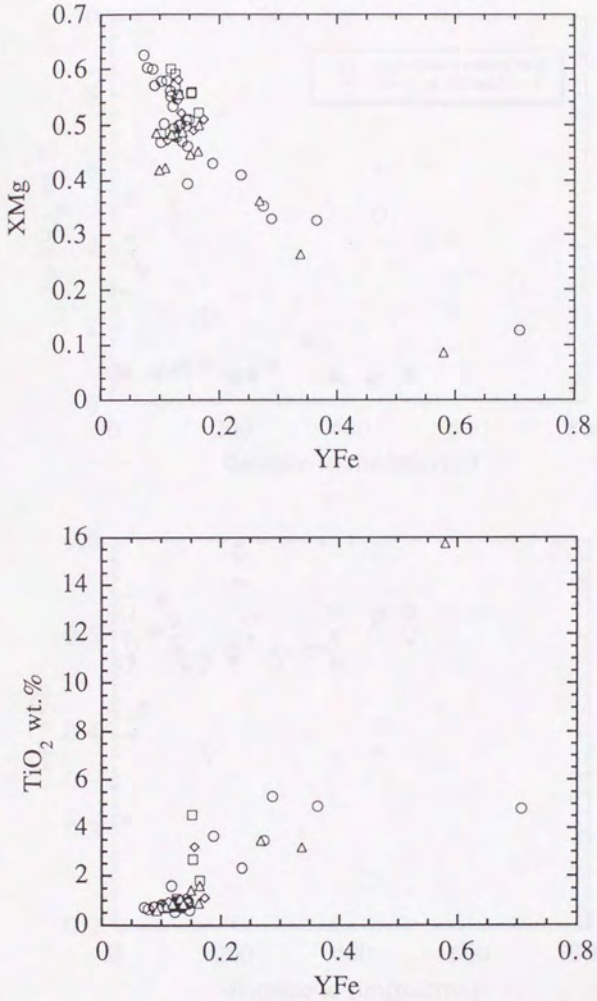

Fig.3-3 Chemical variations of core of spinel.(Continued)

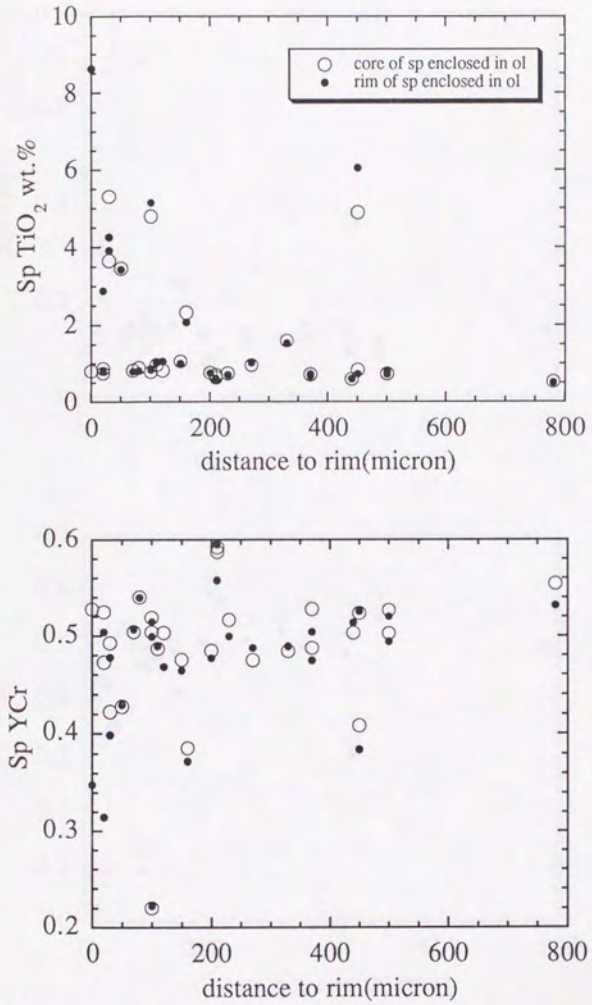

Fig.3-4 Chemical variation of spinel enclosed in olivine. Correlation between distance to the rim of host olivine and spinel chemistry: open circle; core of spinel, filled circle; rim of spinel

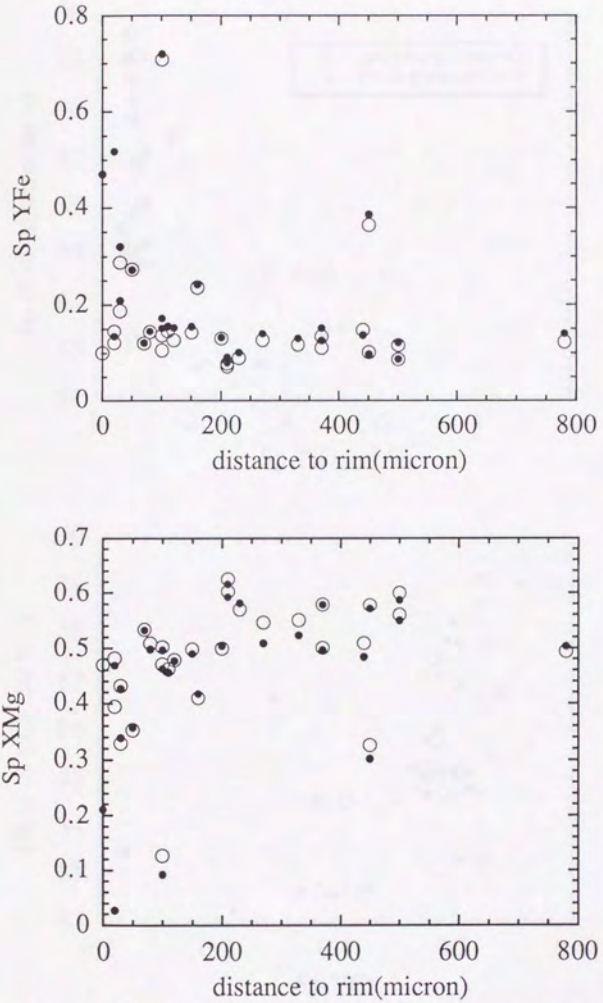

Fig.3-4 Correlation between distance to the rim of host olivine and spinel chemistry.(Continued)

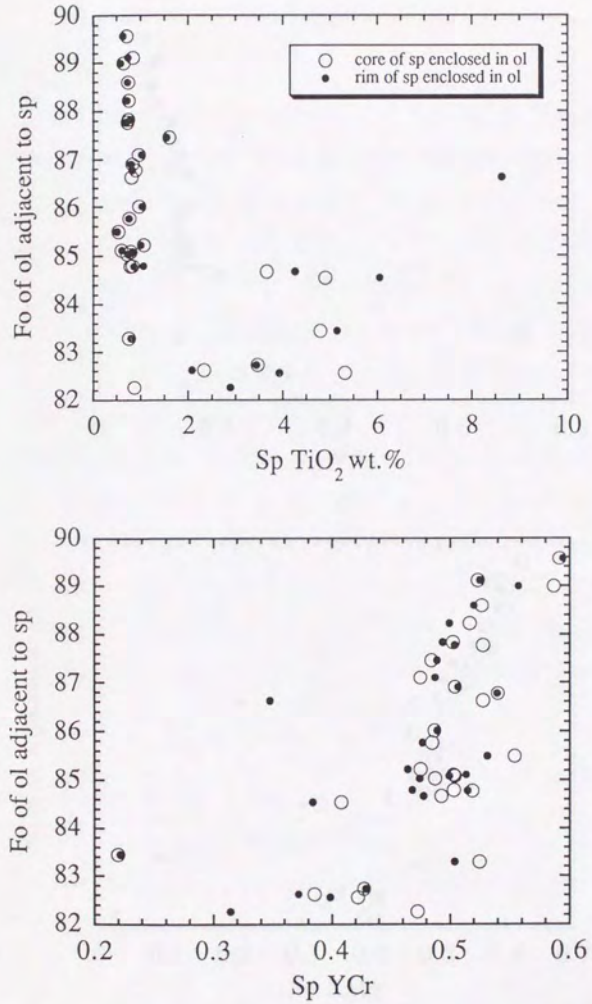

Fig.3-5 Chemical variation of spinel enclosed in olivine and adjacent olivine Fo content: open circle; core of spinel, filled circle; rim of spinel

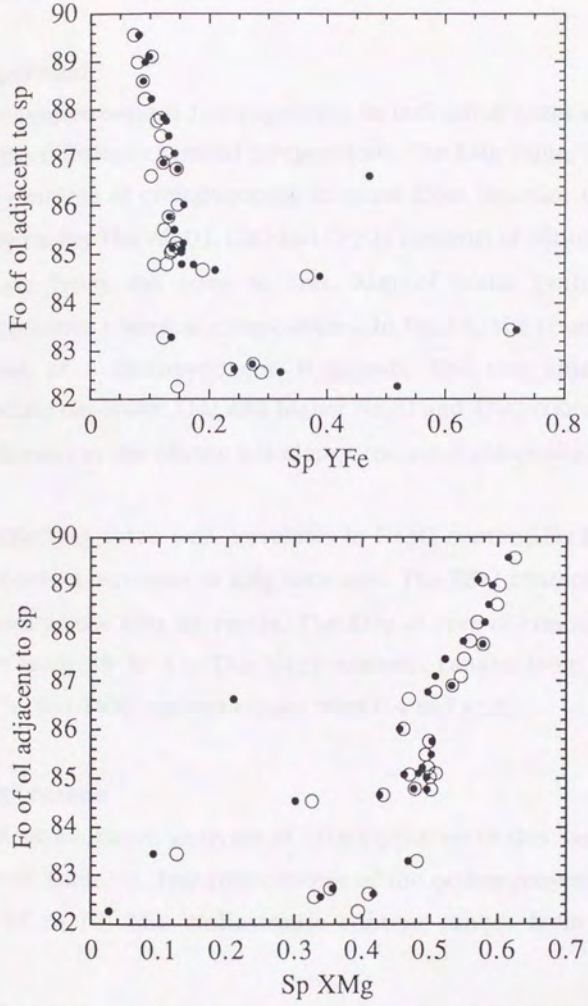

Fig.3-5 Chemical variation of spinel enclosed in olivine and adjacent olivine Fo content.(Continued)

with some very high value. The similar tendency is also exhibited for YCr, YFe and XMg(Fig.3-5).

Clinopyroxene

Clinopyroxene is heterogeneous in individual grain and each grain has different chemical compositions. The XMg value, TiO_2 and Na_2O contents of clinopyroxene increase from the core to rim of clinopyroxene. The Al_2O_3, CaO and Cr_2O_3 contents of clinopyroxene decrease from the core to rim. Rim of some grains show heterogeneous chemical compositions. In Fig.3-6, the result of line analyses of a clinopyroxene is shown. The rim adjacent to plagioclase has lower XMg and higher Na_2O and TiO_2 contents. The rim adjacent to the olivine has almost the same composition as the core.

The XMg value well correlates to Na_2O content(Fig3-7). The Na_2O content increases as XMg decreases. The TiO2 content slightly increases as the XMg decreases. The XMg of core of clinopyroxene ranges from 89 to 81. The Na_2O content ranges from 0.18 to 0.4wt.%. The TiO_2 content ranges from 0.4 to 1wt.%.

Orthopyroxene

Representative analyses of orthopyroxene of this sample are shown in Table3-1. Enstatite content of the orthopyroxene ranges from 85 to 76. The Wollastonite content ranges from 4 to 1.

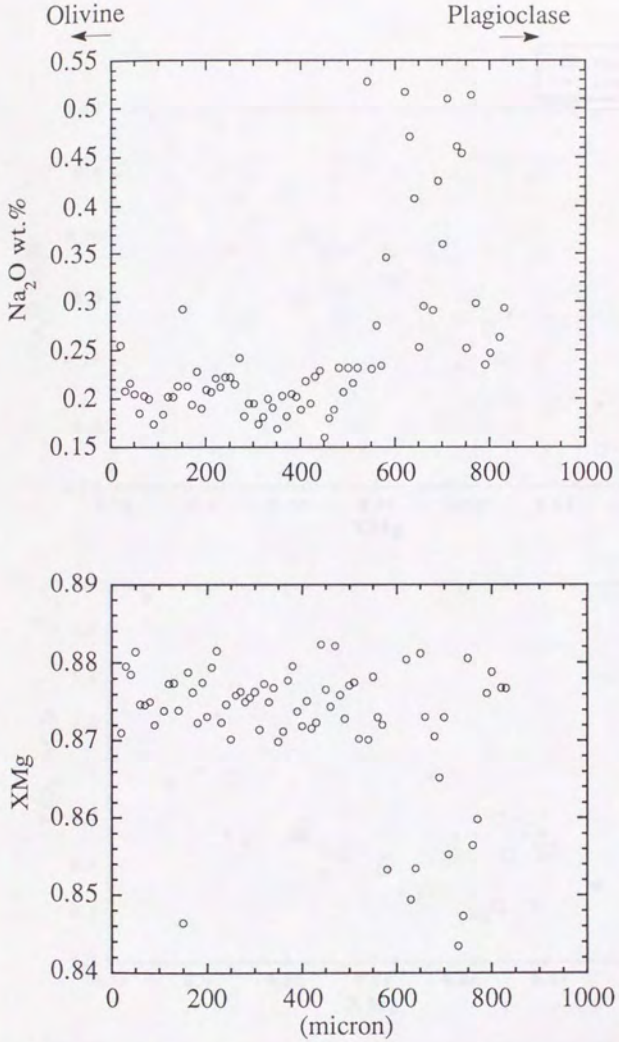

Fig.3-6 Line analyses of clinopyroxene in the olivine orthocumulate. Scan step is 10 micron. Note heterogeneous rim composition.

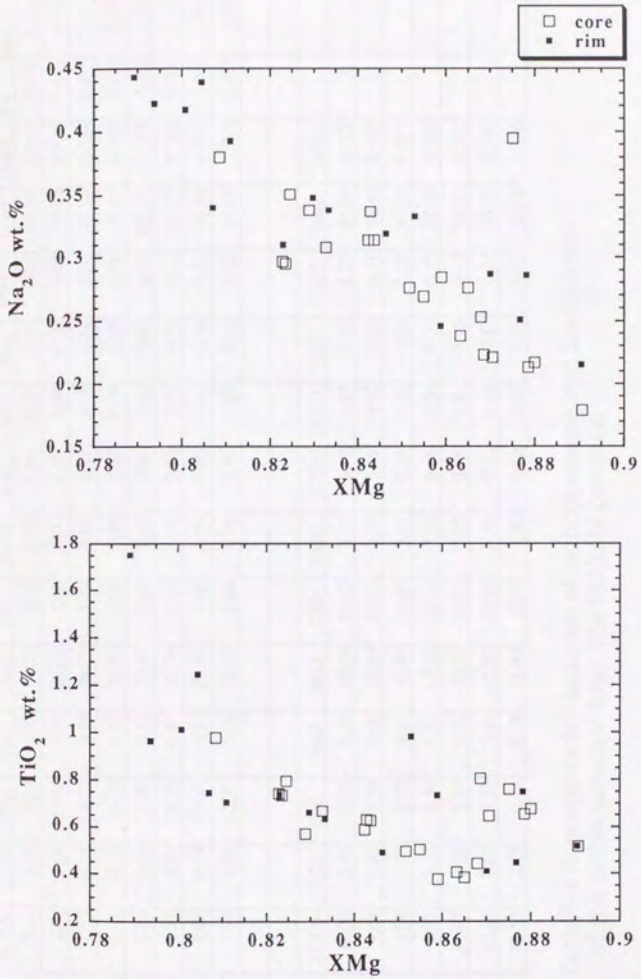

Fig.3-7 Chemical variation of clinopyroxene. Na_2O and TiO_2 correlate to XMg: open square; core, filled square; rim

Orthopyroxene																	
Sample No.	SiO2	Al2O3	TiO2	FeO	MnO	MgO	CaO	Na2O	K2O	Cr2O3	NiO	V2O3	Total	XMg	Wo	En	Fs
opx R36 MYN2	54.25	3.10	0.03	8.42	0.23	31.23	0.95	0.03	0.00	0.08	0.16	0.03	98.50	0.869	0.019	0.852	0.129
opx C39 MYN2	52.89	2.11	0.60	12.82	0.41	28.01	1.66	0.06	0.00	0.08	0.10	0.07	98.80	0.796	0.033	0.770	0.198
opx C206 MYN2	54.08	1.52	0.31	13.75	0.33	28.27	0.79	0.02	0.01	0.06	0.14	0.00	99.28	0.786	0.015	0.773	0.211
opx R207MYN2	53.66	1.48	0.25	14.26	0.38	28.97	0.68	0.02	0.02	0.04	0.08	0.04	99.87	0.784	0.013	0.773	0.214
opx C210 MYN2	53.70	2.29	0.23	13.68	0.37	29.47	0.49	0.03	0.00	0.00	0.00	0.04	100.30	0.793	0.009	0.786	0.205
opx R211 MYN2	54.18	1.11	0.21	13.79	0.43	28.79	0.49	0.01	0.00	0.04	0.11	0.02	99.17	0.788	0.009	0.781	0.210
opx C219 MYN2	53.55	2.02	0.59	12.77	0.34	27.87	2.09	0.03	0.00	0.07	0.10	0.05	99.49	0.795	0.041	0.763	0.196
opx R220 MYN2	53.02	1.94	0.50	12.77	0.36	28.02	1.60	0.03	0.00	0.07	0.15	0.02	98.49	0.796	0.032	0.771	0.197
Hornblende																	
Sample No.	SiO2	Al2O3	TiO2	FeO	MnO	MgO	CaO	Na2O	K2O	Cr2O3	NiO	V2O3	Total	XMg			
hb C21 MYN2	42.94	10.34	3.43	8.95	0.14	16.09	10.62	3.10	0.19	0.05	0.02	0.27	96.14	0.762			
hb R22 MYN2	44.97	9.64	1.62	9.04	0.08	16.83	10.93	2.79	0.26	0.02	0.12	0.11	96.40	0.768			
hb C25 MYN2	43.01	9.99	3.55	8.70	0.17	16.47	10.48	3.07	0.20	0.08	0.08	0.18	95.97	0.771			
hb R26 MYN2	47.28	6.77	2.28	8.56	0.18	17.25	10.12	2.33	0.15	0.06	0.01	0.15	95.14	0.782			
hb C43 MYN2	42.33	11.11	3.08	9.47	0.18	15.66	10.73	2.99	0.16	0.01	0.12	0.13	95.97	0.747			
hb R44 MYN2	42.92	10.76	2.63	9.51	0.16	15.91	10.55	3.06	0.21	0.01	0.17	0.16	96.05	0.749			
hb 205SP203-204	42.92	10.55	2.93	10.14	0.18	15.85	10.90	3.00	0.20	0.03	0.12	0.17	96.98	0.736			

Table3-1 Representative analyses of orthopyroxene and hornblende of the orthocumulate from the Mikkabi complex.

Hornblende

Representative analyses of hornblende of this sample are shown in Table3-1. The XMg value ranges from 78 to 74. The Al_2O_3 and TiO_2 contents decrease from the core to rim.

Geothermometry

In Fig.3-8, calculated temperatures of this rock are shown. The temperatures of two pyroxenes are calculated by the method of Wells(1977). Average temperature is 1050°C. The temperatures of olivine-spinel are calculated by the method of Fabriès(1979). Average temperature is 1000°C. According to olivine-spinel geospeedmetry of Ozawa(1984), cooling rate of this rock ranges from 1000°C to 100°C per year.

5. Discussion

Interstitial liquid fractionation

According to the shape and XMg values of minerals, crystallization order of this rock can be determined. Olivine and spinel first crystallized as cumulus phases. Clinopyroxene crystallized in interstices of olivine. Orthopyroxene follows clinopyroxene. Finally, hornblende, phlogopite and ilmenite crystallized. Modal composition of interstitial minerals is 36%. Some olivine and spinel may crystallize after accumulation. If the system is assumed to be closed after accumulation, this sample first probably contains about 36% of liquid at least. Now interstitial liquid evolution is considered.

Chemical variation in the orthocumulate from the Mikkabi complex suggests Fe-trend and increase of Ti strongly correlates to trapped liquid fractionation with relatively low and narrow range

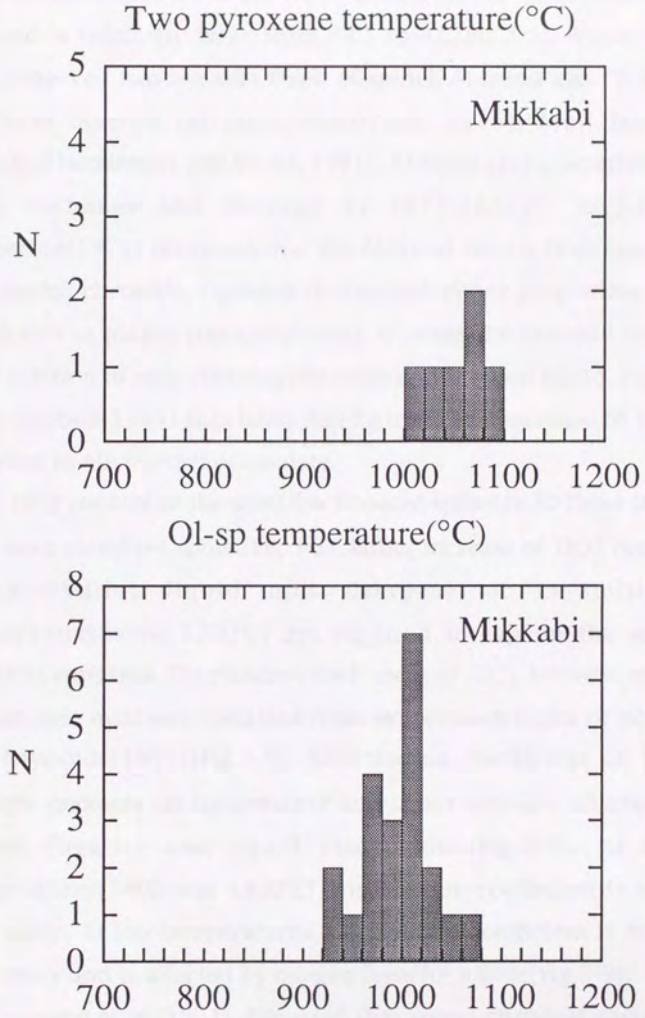

Fig.3-8 Temperatures of two pyroxenes calculated by the method of Wells(1977) and those of olivine-spinel calculated by the method of Fabriès(1979).

of Fo content(from 85 to 82, Fig.3-5). Decrease of Fo content with Al-trend is relatively large(from 89.5 to 82, Fig.3-5). There have been observed two reaction trend of spinel, Al-trend and Cr-trend in Rhum layered intrusion(Henderson, 1975), Mull layered intrusion(Henderson and Wood, 1981). Al-trend is characterized by Al-Cr exchange and Fe-trend by Fe^{3+}-(Al,Cr) exchange. Henderson(1975) proposed that the Al-trend results from reaction of cumulus chromite, cumulus olivine and either plagioclase or a liquid rich in plagioclase component, whereas the Fe-trend results from reaction of only cumulus chromite and trapped liquid. Roeder and Campbell(1985) suggested that Fe-trend and increase of Ti are observed in olivine orthocumulate.

TiO_2 content of the most fractionated spinel is 30 times larger than most primitive spinel(Fig.3-3). Either increase of TiO2 content in interstitial liquid and decrease of crystallizing temperature(below 1200°C) are required to explain the spinel chemical variation. Distribution coefficient of TiO_2 between spinel and basaltic melt was compiled from experimental data of Roeder and Reynolds(1991)(Fig.3-9). Distribution coefficient of TiO_2 strongly depends on temperature and is not strongly affected by oxygen fugacity and liquid composition(Fig.3-9). At high temperatures(1400 and 1300°C), distribution coefficient is lower than unity. At low temperatures, distribution coefficient is higher than unity and is affected by oxygen fugacity a little(Fig.3-9).

Scowen et al.(1991) discussed that spinel chemical variation in olivine is controlled by chemical diffusion of certain elements from interstitial liquid through olivine. Their estimated diffusion coefficient of Fe^{3+} and Al in olivine is one or two orders magnitude larger than diffusion coefficient of Cr and Ti. Spinel enclosed in

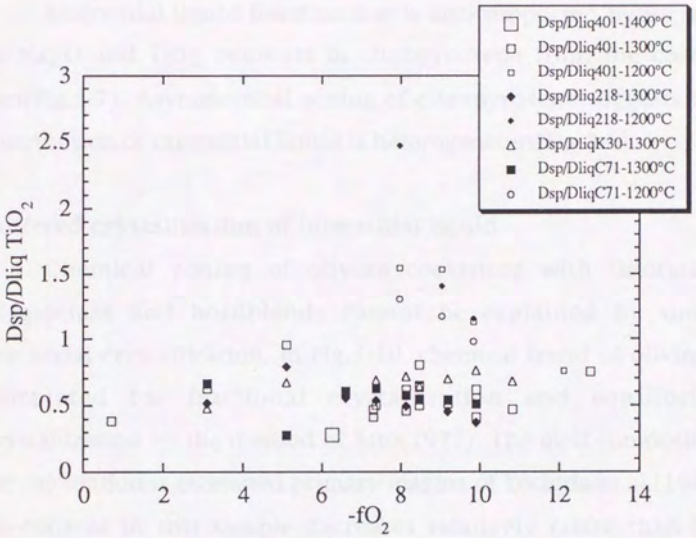

Fig.3-9 Distribution coefficient of TiO_2 between spinel and basaltic melt. Compiled from the experiment of Roeder&Reynolds(1991).

olivine, which has high YFe and low TiO2, has not been observed in this orthocumulate(Fig.3-3). This suggests that chemical diffusion through the olivine did not play an important role for modification of Ti and YFe in the orthocumulate of Mikkabi complex.

Interstitial liquid fractionation is also supported by increase of Na_2O and TiO_2 contents in clinopyroxene from the core to rim(Fig.3-7). Asymmetrical zoning of clinopyroxene suggests that distribution of interstitial liquid is heterogeneous(Fig.3-6).

Buffered crystallization of interstitial liquid

Chemical zoning of olivine coexisting with interstitial plagioclase and hornblende cannot be explained by simple fractional crystallization. In Fig.3-10, chemical trend of olivine is calculated for fractional crystallization and equilibrium crystallization by the method of Sato(1977). The melt composition for calculation is estimated primary magma of Yoshida et al.(1984). Fo content in this sample decreases relatively faster than NiO content decreases whereas calculated NiO content decreases faster than Fo content. Chemical zoning of olivine in this sample cannot be explained by simple fractional crystallization(Fig3-10). NiO content decreases faster than Forsterite content in this sample(Fig.3-2).

Concave compositional profiles of olivine(Fig.3-2) suggest that interstitial liquid was crystallized being buffered by olivine. In the calculation of fractional crystallization, diffusion in olivine was ignored. In the case of crystallization of interstitial liquid in olivine cumulate, the diffusion cannot be ignored because diffusion in olivine is thought to be faster than crystallization of interstitial liquid and because volume of interstitial melt is lower and is easily affected by the diffusion controlled reaction. Diffusion distance $\sqrt{Dt}$

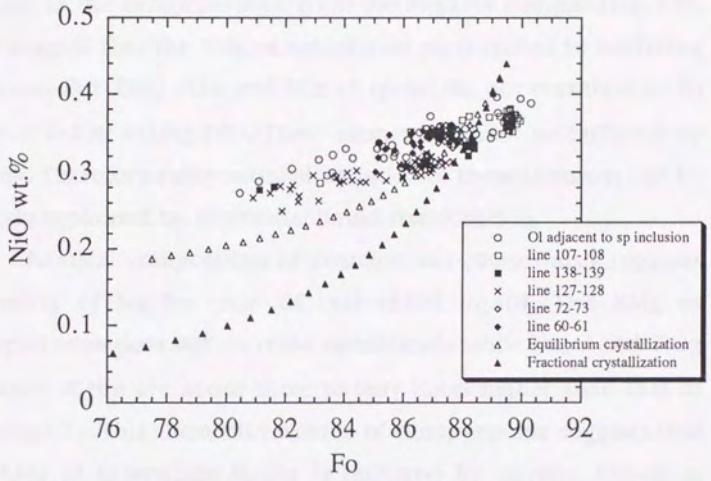

Fig.3-10 Calculated crystallization trends of olivine according to Sato(1977) with the measured composition. Step of calculation is 1%: open circle; equilibrium crystallization, filled circle; fractional crystallization. The melt composition is assumed as the primary magma composition estimated by Yoshida et al.(1984).

of olivine is calculated according to Morioka(1981)'s coefficient. Diffusion distance at 1200°C is about 0.001mm for 0.1 year and 0.1mm for 1 year. It may be comparable to growth of olivine in cumulate.

The XMg of spinel enclosed in olivine well correlates to Fo content in the orthocumulate from the Mikkabi complex(Fig.3-5). This suggest that the XMg of spinel also participated in buffering reaction. But TiO_2, YFe and YCr of spinel do not correlate to Fo content below 85(Fig.3-5). These elements cannot be buffered by olivine. Therefore compositional variation of these elements can be directly explained by interstitial liquid fractionation.

Chemical composition of postcumulus phases also suggests buffering of Mg/Fe ratio of interstitial liquid. The XMg of clinopyroxene does not decrease significantly while Na_2O and TiO_2 contents of rim are about three to four times higher than that of core(Fig3-7). This chemical variation of clinopyroxene suggests that the XMg of interstitial liquid is buffered by olivine. Meyer et al.(1989) proposed that buffered crystallization of interstitial clinopyroxene can explain high TiO_2 content of magnesian clinopyroxene of cumulate gabbro from the Southwest Indian Ridge.

Implication for layered intrusion

The chemical variation of spinel even in one thin section is observed in orthocumulate with homogeneous olivine(e.g. Jimberlana intrusion; Roeder and Campbell, 1985). Chemical variation of spinel suggests that there should be strong chemical variation in olivine of orthocumulate when they crystallized. The variation was caused by trapped liquid crystallization. Chemical composition of cumulus olivine is greatly affected by subsolidus

cooling and does not directly indicate liquidus composition. Barnes(1986) mentioned that trapped liquid crystallization affects chemical composition of olivine. Subsolidus diffusion homogenizes zoned olivine and chemical composition of olivine shifts.

Recently calculation of boundary layer fractionation was done by Langmuir(1989) and Nielsen and DeLong(1992). In general, it is probable that interstitial liquid of olivine matrix after postcumulus phases partly crystallized is buffered by olivine component but has relatively high concentration of incompatible elements. These interstitial liquids have a potential to increase incompatible element concentration without large decrease of compatible elements such as Ni. If interstitial melt is relatively lighter than primitive melt, migration of the melt can occur. Migration of these melts through the cumulus pile can be only observed by increase of the incompatible elements in spinel or clinopyroxene without strong decrease of compatible element concentration. If these melts can move back to main chamber from boundary layer crystal mush, boundary layer fractionation can occur. Calculation of boundary layer fractionation has to consider buffered effect of matrix when melt movement velocity through matrix is lower than diffusion.

IV Petrology of the Toba ultramafic complex

1. Introduction

Chemical compositions of olivine in cumulates have been used to understand the processes in magma chambers for olivine cumulate. The size of magma batch for olivine cumulate is estimated by olivine chemistry because olivine is main cumulus phase and Fo-NiO systematics is well known for fractional crystallization(e.g. Sato, 1977). The thickness of the magma column for the olivine cumulate was determined by the chemical variation of olivine and the thickness of units(Browning, 1984; Wilson, 1982). Wave length of chemical variation of olivine is from 50m to a few hundred meters(e.g. Irvine, 1980; Wilson, 1982). Homogeneous olivine layer up to 50m is considered as a product of equilibrium crystallization from a single magma batch.(Huppert and Sparks, 1980; Tait, 1985).

Chemical composition of olivine is affected by many processes during solidification of liquid and subsolidus cooling. Interstitial liquid crystallization in olivine orthocumulate has a potential to shift olivine chemistry. Barnes(1986) pointed out that chemical composition of olivine is not only determined by fractional crystallization from liquid but also by interstitial crystallization and subsolidus diffusion. Subsolidus reequilibration with other phases also has to be considered. At this time chemical composition of other phases also change. XMg values of clinopyroxene and spinel also shift(e.g. Obata et al., 1974; Ozawa, 1984).

In this chapter, the mineral chemistry of the Toba ultramafic complex is discribed and heterogeneous chemical composition of spinel in olivine cumulate is shown to be interstitial liquid

crystallization. Also subsolidus reequilibration of olivine and clinopyroxene is discussed and cooling rate is estimated from degree of homogenization of olivine, clinopyroxene and spinel. After that I will present some comments to the mineral chemical composition of oceanic gabbros.

2. Mineral chemistry of the Toba ultramafic complex

Olivine

Olivine of Unit I is homogeneous in each grain and each sample. The range of variation of Fo content within each sample is less than 1.5. The average Fo content for each sample ranges from 87.9 to 80.7(Table 2-1). Olivine in olivine cumulate is generally more magnesian than that in olivine clinopyroxene cumulate. The most magnesian olivine occurs in the western part of the mass, which is supposed to correspond to a relatively lower horizon. Any large scale systematic stratigraphic variation is not observed. The CaO content of olivine is typically less than 0.06wt.%. The CaO content in the most magnesian olivine is higher than this value and attains 0.1wt.%. The NiO content ranges from 0.34 to 0.25wt.% and the MnO content ranges from 0.32 to 0.19Wt.%(Fig.4-1).

Only two specimens from Unit II contain relict olivine, which is also homogeneous in each grain and each sample. Olivine in olivine hornblendite shows bimodal grain size distribution, but there is no difference in Fo content between them. Their Fo content ranges from 84.8 to 78.4(Fig.4-1). The CaO content of olivine is less than 0.05wt.%. The NiO content ranges from 0.37 to 0.32wt.% and the MnO content ranges from 0.29 to 0.23wt.%.

Only three specimens of Unit III contain relict olivine. The chemical variation of olivine is wider than that of Unit I and Unit II.

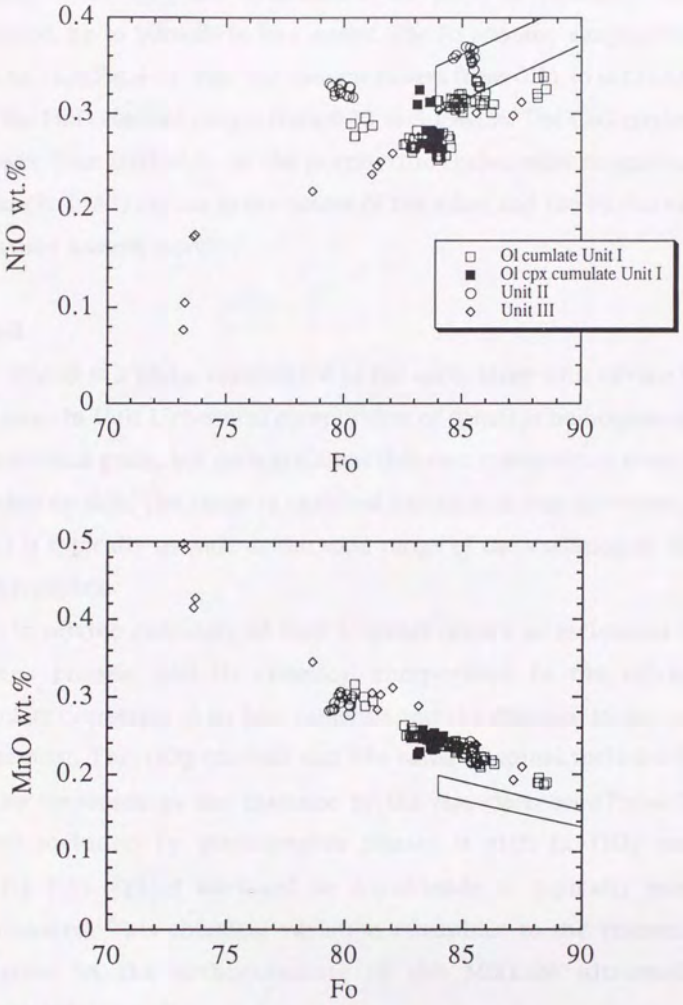

Fig.4-1 Chemical variation of olivine in the Toba ultramafic complex: open square; ol cumulate of Unit I, filled square; olivine clinopyroxene cumulate of Unit I, open circle; Unit II, open diamond; Unit III. The box indicates the mantle olivine array of Takahashi et al.(1987).

Some olivine grains have chemical zoning up to 6mol% in Fo content. Grain by grain variations in the same specimen are also observed, up to 10mol% in Fo content. The Fo content ranges from 87.2 to 71.5(Fig.4-1). The NiO content ranges from 0.31 to 0.17wt.%, and the MnO content ranges from 0.43 to 0.19wt.%. The CaO content is lower than 0.05wt.%. In the porphyritic rocks, most magnesian olivine(Fo is 87) occurs in the center of the dikes and the Fo content decreases toward margin.

Spinel

Spinel is a phase crystallized in the early stage with olivine in all units. In Unit I, chemical composition of spinel is homogeneous in individual grain, but each grain has different composition even in one thin section. The range of chemical variation in one specimen in Unit I is typically as wide as the total range of the variation in the Toba complex.

In olivine cumulate of Unit I, spinel occurs as inclusions in various phases, and its chemical composition in the olivine cumulate correlates to its host minerals and the distance to the rim of the host. The TiO_2 content and YFe value of spinel included in olivine increases as the distance to the rim decreases(Fig.4-2). Spinel included by postcumulus phases is rich in TiO_2 and YFe(Fig.4-3). Spinel enclosed in hornblende is typically most fractionated. This chemical variation resembles to the chemical variation in the orthocumulate of the Mikkabi ultramafic complex(Chapter III).

Chemical composition of spinel and host olivine chemistry are examined in Fig.4-4. In olivine cumulate of Unit I, the TiO_2 and YFe of spinel enclosed in olivine increase, and the YCr and XMg of spinel

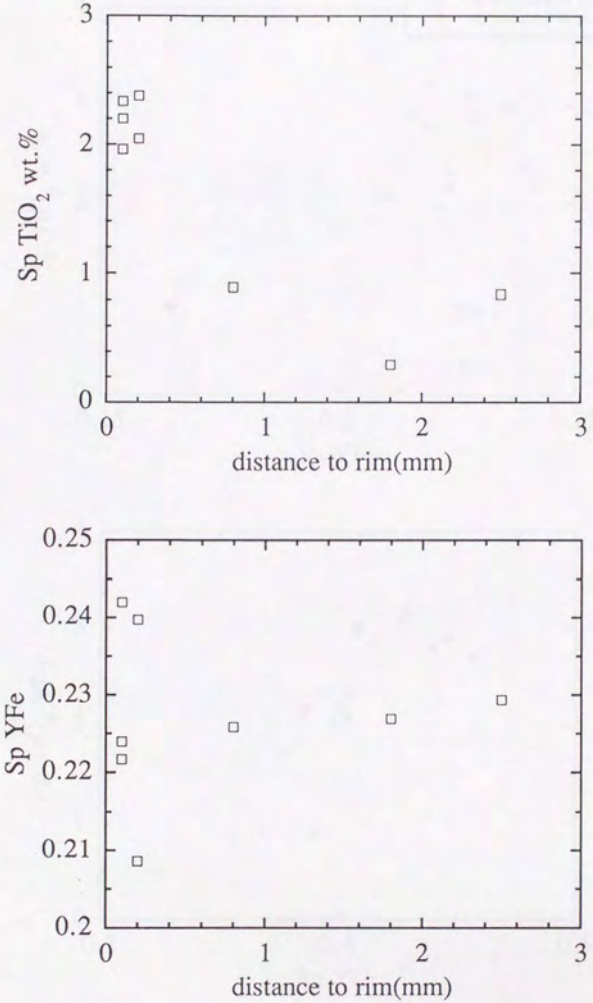

Fig.4-2 Chemical variation of spinel core enclosed in olivine of a olivine cumulate in Unit I(T221410). Distance to the rim of host olivine correlates to TiO_2 and YFe.

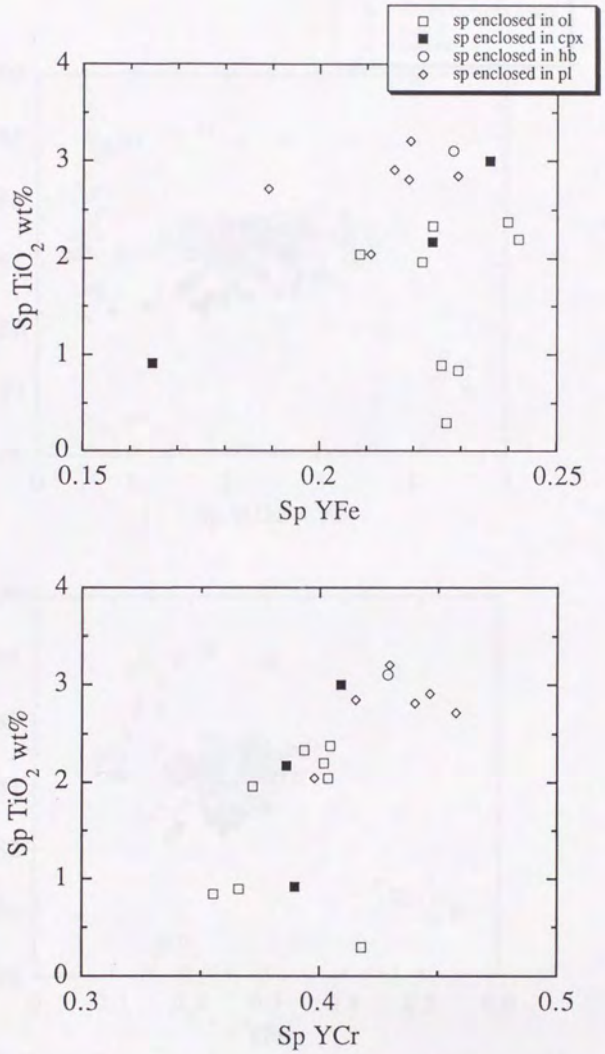

Fig.4-3 Chemical variation of spinel core and its enclosing minerals in a olivine cumulate of Unit I(T221410): open square; spinel enclosed in olivine, filled square; spinel enclosed in clinopyroxene, open circle; spinel enclosed in hornblende, open diamond; spinel enclosed in plagioclase.

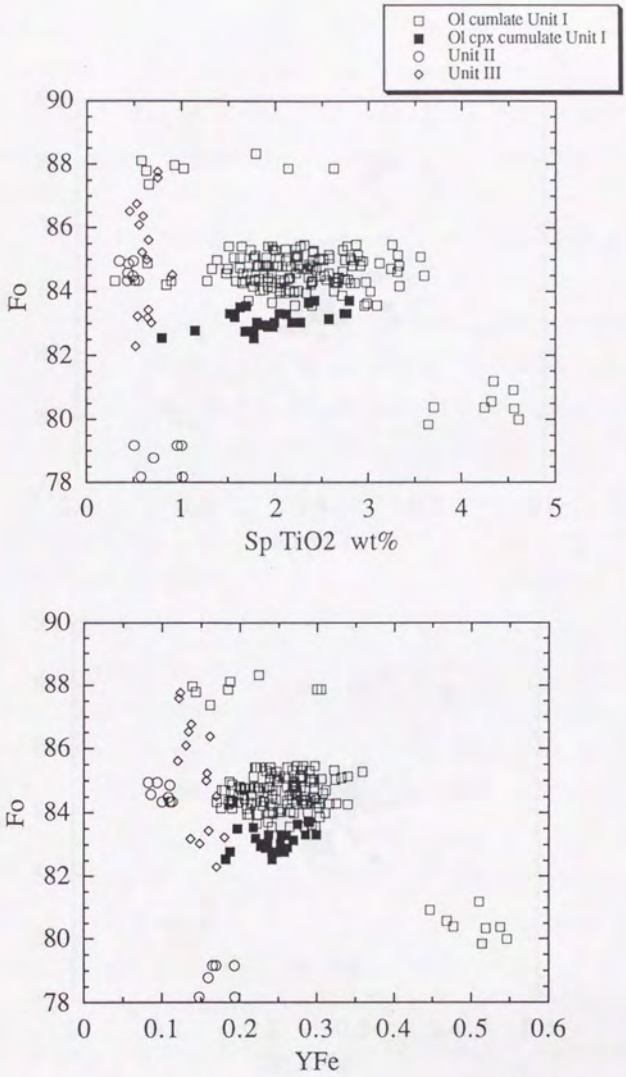

Fig.4-4 Chemical variation of spinel and host olivine Fo content of the Toba ultramafic complex. The symbols are similar to Fig.4-1.

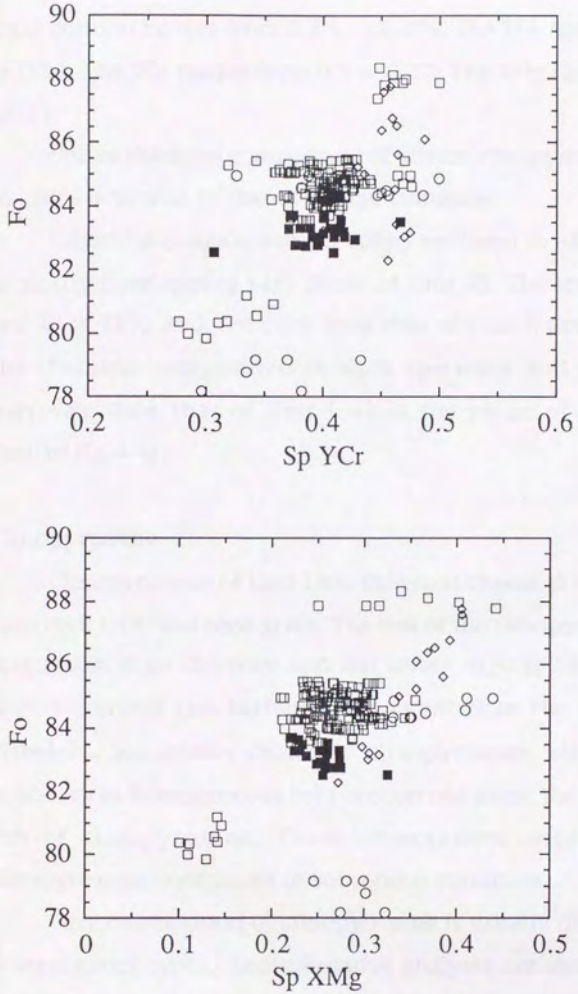

Fig.4-4 Chemical variation of spinel and host olivine Fo content of the Toba ultramafic complex.(Continued)

decrease as Fo content of host olivine decreases. But chemical composition of spinel is more heterogeneous than that of olivine. TiO2 content ranges from 0.2 to 4.6wt%. The YFe ranges from 0.13 to 0.54. The YCr ranges from 0.5 to 0.27. The XMg ranges from 0.44 to 0.1.

Spinel chemical composition of olivine clinopyroxene cumulate in Unit I is similar to that of olivine cumulate.

Chemical compositions of spinel enclosed in olivine of Unit II is mostly overlapping with those of Unit III. The spinel in Unit II and III is TiO_2 and YFe poor than that of Unit I, and the range of the chemical composition in each specimen and as a whole is narrower than that of Unit I while the range of Fo content is similar(Fig.4-4).

Clinopyroxene

Clinopyroxene of Unit I has different chemical composition in each rock type and each grain. The rim of the clinopyroxene is more magnesian than the core and has lower Al_2O_3, TiO_2, Na_2O and Cr_2O_3 content and higher CaO content than the core(Plate4-1, Plate4-2). Sometimes diopsidic clinopyroxene with very sharp boundary to homogeneous core is observed along the discontinuous rim of clinopyroxene. These observations suggest diopsidic clinopyroxene crystallizes in subsolidus condition.

Core composition of clinopyroxene is usually different among different rock types. Representative analyses are shown in Table4-1. Clinopyroxene of olivine cumulate is anhedral, occurs in interstices as a post cumulus phase. Whereas the clinopyroxene of olivine clinopyroxene cumulate is euhedral and a cumulus phase. The core of cumulus clinopyroxene is less magnesian than the core

Clinopyroxene	Sample No.	SiO2	Al2O3	TiO2	FeO	MnO	MgO	CaO	Na2O	K2O	Cr2O3	NiO	V2O5	Total	XMg	Calc. Fe2O3	Calc. FeO	Recal XMg
Unit I																		
Ol cumulate	T541410 C1	51.59	3.83	0.62	3.42	0.12	15.54	23.01	0.49	0.01	1.11	0.03	0.01	99.78	0.890	0.83	2.68	0.912
Ol cumulate	T54141O C2	51.30	3.76	0.60	3.46	0.09	15.64	22.87	0.42	0.00	1.01	0.00	0.01	99.16	0.890	0.88	2.67	0.913
Ol cumulate	T051410 C1	51.54	3.76	0.76	3.97	0.08	15.42	23.08	0.49	0.00	0.93	0.00	0.04	100.07	0.874	1.18	2.91	0.904
Ol cumulate	T051410 C2	51.56	3.67	0.77	4.07	0.12	15.23	23.42	0.45	0.03	1.01	0.00	0.08	100.41	0.870	1.20	2.99	0.901
Ol cpx cumlate	T011510 C1	51.07	4.38	0.69	4.57	0.14	15.72	22.69	0.31	0.01	0.71	0.03	0.06	100.38	0.860	1.72	3.02	0.903
Ol cpx cumlate	T011510 C2	51.56	4.22	0.60	5.48	0.15	14.60	23.01	0.45	0.00	0.70	0.09	0.06	100.92	0.826	1.14	4.45	0.854
Ol cpx cumlate	T141510 C1	50.98	4.42	0.67	5.72	0.11	16.19	21.23	0.32	0.01	0.86	0.04	0.04	100.59	0.835	2.01	3.91	0.881
Ol cpx cumlate	T141510 C2	51.49	3.73	0.54	4.92	0.14	15.22	23.29	0.32	0.02	0.62	0.00	0.05	100.34	0.846	1.62	3.46	0.887
Unit II																		
C.cpx-hb-gabbro	T012711C C1	53.18	0.92	0.10	8.25	0.32	14.18	23.12	0.25	0.01	0.04	0.00	0.00	100.37	0.754			
C.cpx-hb-gabbro	T012711C C2	53.16	0.58	0.08	7.46	0.29	14.22	23.85	0.20	0.02	0.03	0.00	0.00	99.89	0.773			
F.cpx-hb-gabbro	T062611A C1	53.56	0.91	0.17	9.89	0.39	13.04	22.25	0.25	0.01	0.03	0.00	0.00	100.50	0.701			
F.cpx-hb-gabbro	T062611A C2	53.04	0.92	0.14	10.15	0.33	13.36	22.11	0.28	0.00	0.00	0.00	0.00	100.33	0.701			
Unit III																		
Ol-cpx-hb-gabbro	T02263B	53.43	1.18	0.28	5.60	0.21	15.75	23.03	0.28	0.00	0.00	0.03	0.00	99.79	0.834			
Ol-cpx-hb-gabbro	T02263B	53.26	1.92	0.33	6.29	0.23	15.00	23.08	0.39	0.00	0.18	0.03	0.00	100.71	0.809			
F.cpx-hb-gabbro	T01297	52.20	0.94	0.17	9.45	0.28	13.87	21.56	0.24	0.01	0.00	0.03	0.07	98.82	0.723			
F.cpx-hb-gabbro	T01297	52.10	1.09	0.29	9.96	0.39	13.53	21.51	0.29	0.02	0.00	0.02	0.02	99.22	0.708			

Table4-1 Representative analyses of clinopyroxene of the Toba ultramafic complex. Fe_2O_3 content is calculated according to Lindsley and Anderson(1983).

of interstitial clinopyroxene(Fig.4-5). The XMg of cumulus clinopyroxene ranges from 0.89 to 0.826. The XMg of interstitial clinopyroxene ranges from 0.918 to 0.827. Cumulus clinopyroxene has relatively low TiO_2 and Na_2O content(Fig. 4-5). The TiO_2, and Na_2O content of cumulus clinopyroxene ranges from 0.45 to 0.81, 0.22 to 0.5wt.%, respectively. The TiO_2 and Na_2O content of interstitial clinopyroxene ranges from 0.1 to 1.1, 0.1 to 0.79wt.%, respectively.

Clinopyroxene of Unit II is less magnesian than that of Unit I. Representative analyses are shown in Table4-1. The XMg ranges from 0.77 to 0.7. The Al_2O_3, Na_2O and Cr_2O_3 contents are lower than those of clinopyroxene in Unit I. Clinopyroxene of Unit II is homogeneous in each grain and specimen. Coarse-grained clinopyroxene observed in fine grained clinopyroxene hornblende gabbro is not different in chemical composition from fine-grained one.

Clinopyroxene in Unit III is less magnesian than Unit I: the XMg of clinopyroxene ranges from 0.83 to 0.7. The Al_2O_3, TiO_2, Na_2O and Cr_2O_3 contents are relatively lower than Unit I. Representative analyses are shown in Table4-1.

Plagioclase

Only one relict plagioclase can be observed as an inclusion of olivine. The An content is 82.5, and the Fo content of the coexisting olivine is 83.6. The similar range of An and Fo contents(An84, Fo83) of coexisting plagioclase and olivine were reported by Inomata(1979) from the Mikkabi complex.

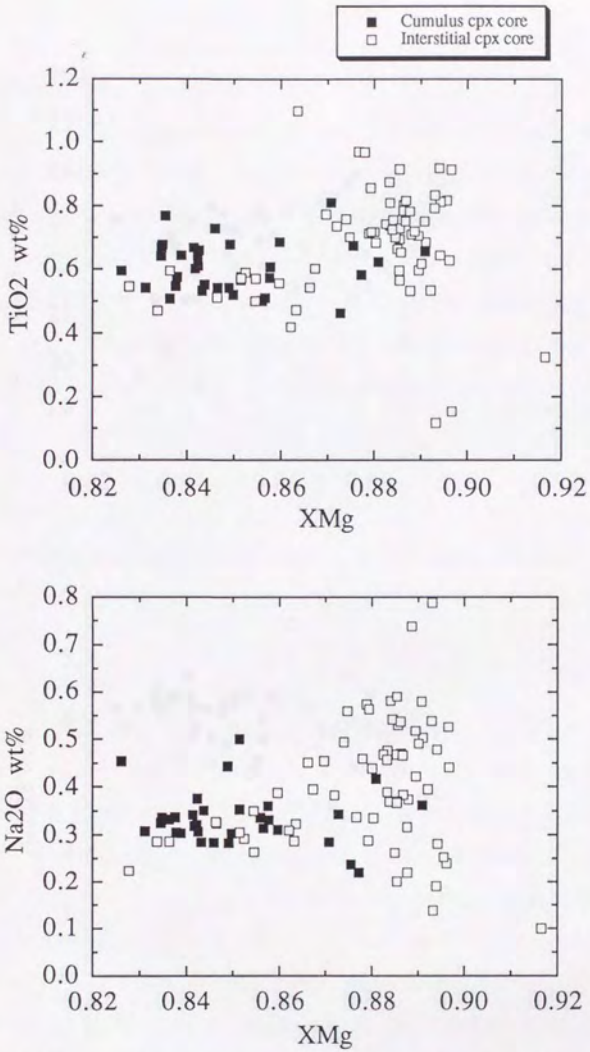

Fig.4-5 Chemical variation of clinopyroxene core in Unit I. closed square; cumulus clinopyroxene, open square; interstitial clinopyroxene.

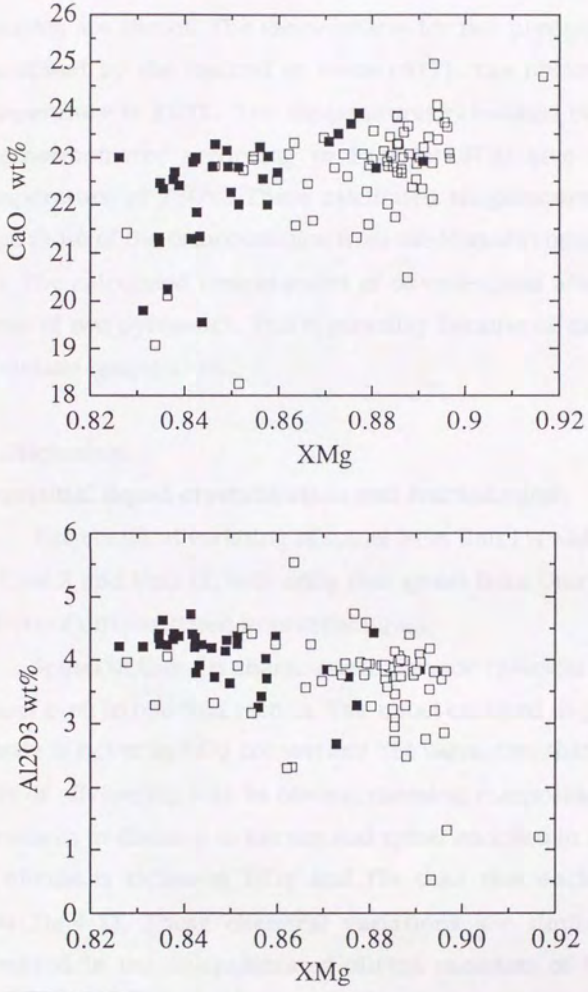

Fig.4-5 Chemical variation of clinopyroxene core in Unit I. (Continued)

Geothermometry

In Fig.4-6, calculated temperatures of the Toba ultramafic complex are shown. The temperatures for two pyroxene pairs are calculated by the method of Wells(1977). The obtained average temperature is 850°C. The temperatures calculated olivine-spinel geothermometer according to Fabriès(1979) give an average temperature of 750°C. These calculated temperatures are lower than those of the orthocumulate from the Mikkabi complex(Chapter III). The calculated temperatures of olivine-spinel are lower than those of two pyroxenes. This is probably because of the difference in closure temperature.

3. Discussion

Interstitial liquid crystallization and fractionation

The chemical variation of spinel from Unit I is wider than that of Unit II and Unit III, indicating that spinel from Unit I preserved effects of differentiated interstitial liquid.

Spinel in Unit I is characterized by wide chemical variation of spinel even in one thin section. The spinel enclosed in postcumulus phases is richer in TiO_2 content and YFe value than that enclosed in core of olivine(Fig.4-3). In olivine, chemical composition of spinel correlates to distance to the rim and spinel enclosed in the rim part of olivine is richer in TiO_2 and YFe than that enclosed in the core(Fig.4-2). These chemical variations are similar to these observed in the unequilibrated olivine cumulate of the Mikkabi complex(Fig.3-3, Fig.3-4; Chapter III) and can be interpreted by the interstitial liquid crystallization and fractionation(Fig.4-7). Enrichment of TiO_2 and YFe content in spinel is caused by enrichment of those components in interstitial liquid(Fig4-7).

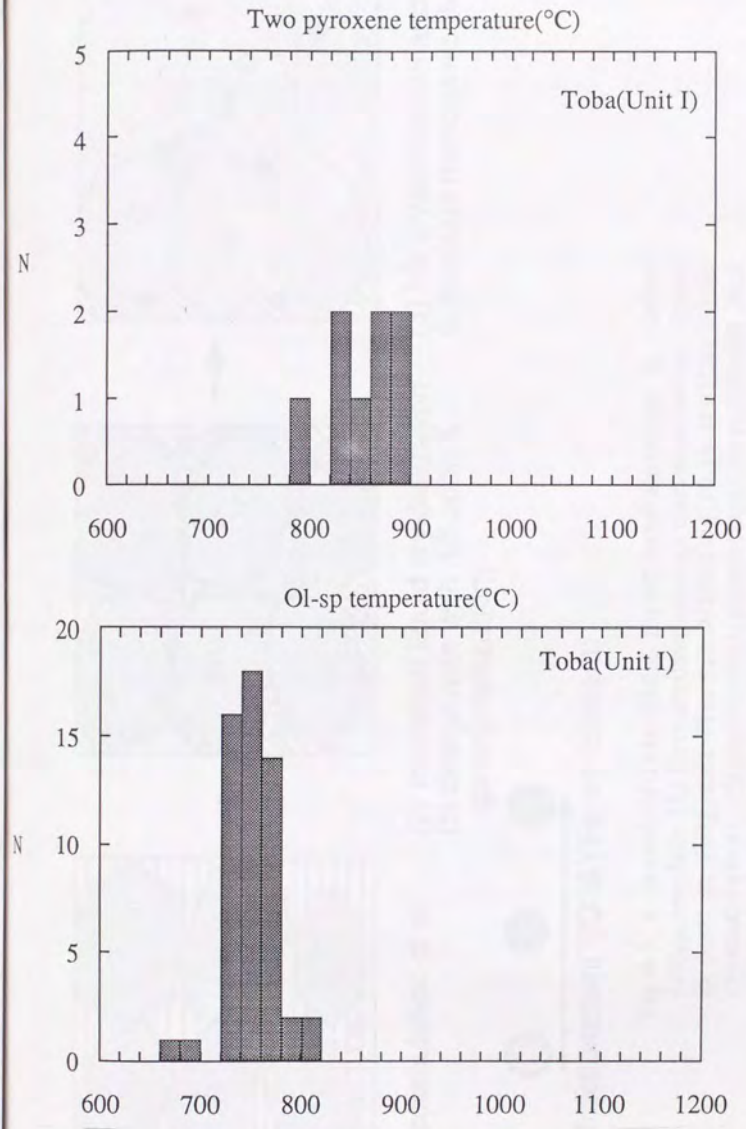

Fig.4-6 Calculated temperatures of two pyroxenes(Wells, 1977) and olivine-spinel(Fabriès, 1979) of Unit I of the Toba ultramafic complex. The temperatures are lower than those of the Mikkabi orthocumulate(Fig.3-8, Chapter III).

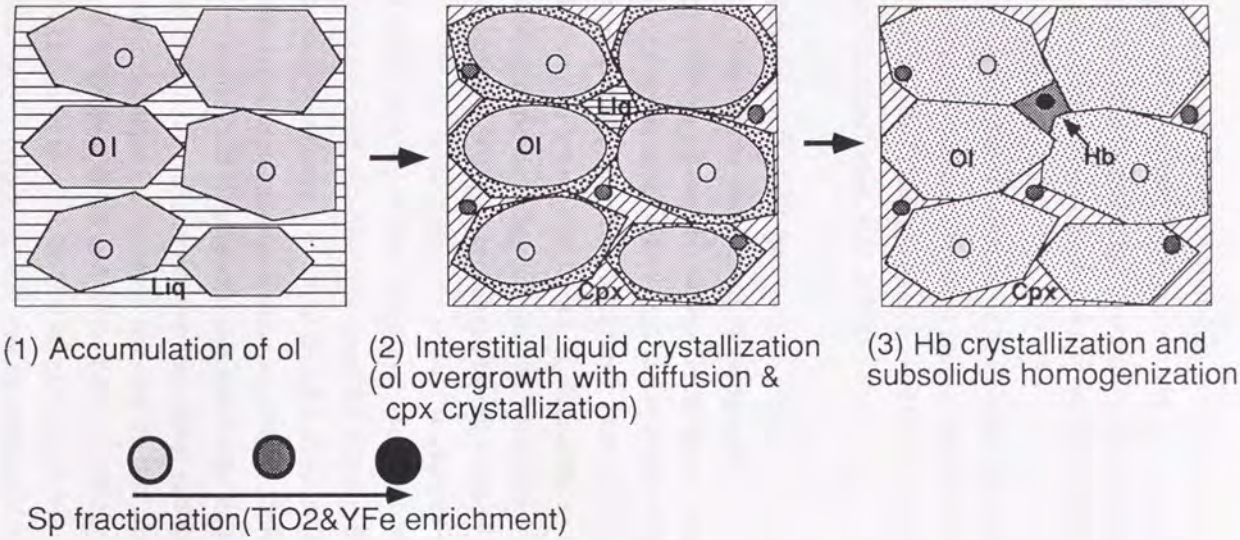

Fig.4-7 A model of interstitial liquid crystallization in olivine orthocumulate. (1) First accumulation of olivine occurred. Spinel is poor in TiO_2 and YFe. (2) According to interstitial liquid crystallization, clinopyroxene(plagioclase) crystallized and overgrowth of olivine occurred. Spinel of this stage became TiO_2 and YFe rich. Diffusion in olivine probably occurred.(3) Finally hornblende crystallized from fractionated interstitial liquid. Spinel is rich in TiO2 and YFe. According to subsolidus diffusion, olivine became homogeneous.

Some of spinel included in interstitial mineral have lower TiO_2 and YFe than those included in rim part of olivine(Fig.4-2, Fig.4-3). This suggests that overgrowth of olivine with inclusions of fractionated spinel occurs even after interstitial phases begin to crystallize.

Interstitial clinopyroxene has higher TiO_2 and Na_2O contents than that of cumulus pyroxene(Fig.4-5). Enrichment of incompatible element in clinopyroxene supports interstitial liquid fractionation(Meyer et al., 1989).

Chemical shift of olivine

The above-mentioned heterogeneity of spinel chemical composition within the same olivine grain suggests interstitial liquid fractionation with overgrowth of olivine(Fig.4-7). In general, chemical composition of overgrowth part of olivine is affected by fractionated interstitial liquid. If diffusivity in olivine is not so rapid, olivine has chemical zoning firstly(Fig.4-7). The average composition of olivine is changed by the overgrowth of olivine.

On the Fo-NiO diagram of olivine, the trend of the Unit I is characterized by flatter signature than that of the calculated fractional and equilibrium crystallization trend(Fig.4-8). The chemical composition of initial liquid is assumed to be 071911A of Table2-2. The calculation is done according to Sato(1977).

Barnes(1986) suggested that interstitial liquid crystallization can change the chemistry of cumulus phase and the element rich in interstitial liquid is strongly affected by this process. In olivine, only Fo content shifts and NiO content is relatively unchangeable. The chemical trend in Fo-NiO diagram of olivine of Unit I in Toba ultramafic complex(Fig.4-8) can be explained by the model of

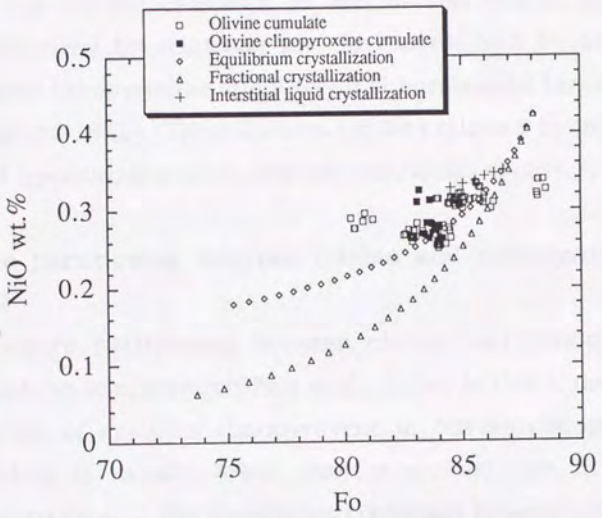

Fig.4-8 Calculated crystallization trends of olivine according to Sato(1977) with measured composition of olivine in Unit I. The calculated step of subtraction is 1%. Primary melt composition is assumed as T071911 of Table2-2: open circle; equilibrium crystallization, closed circle; fractional crystallization. Chemical shifts by interstitial liquid crystallization is calculated according to Barnes(1986). The starting composition of olivine and melt are these of 5% fractional crystallization. The amount of interstitial liquid is varied from 5% to 30% with 5% step; plus.

Barnes(1986). Calculated compositional change by interstitial liquid crystallization is characterized by flatter trend in Forsterite-NiO diagram(Fig.4-8).

The olivine cumulate of the Mikabu belt is generally characterized by relatively low Fo content and by abundant poikilitic clinopyroxene and interstitial hornblende(Tazaki, 1966; Nakamura, 1971). These features can be explained by interstitial liquid crystallization with compositional change of olivine.

Mg-Fe partitioning between olivine and clinopyroxene in Unit I

Mg-Fe partitioning between olivine and clinopyroxene depends on temperature(Obata et al., 1974). In Unit I, the XMg of the core of cumulus clinopyroxene in olivine clinopyroxene cumulate is usually lower than interstitial one in olivine cumulate(Fig.4-5). The distribution coefficient between olivine and clinopyroxene for olivine clinopyroxene cumulate is higher than that for olivine cumulate.

The variation of XMg can not be explained by the contamination of orthopyroxene lamellae during EPMA analysis. If the contamination of orthopyroxene lamellae makes euhedral clinopyroxene less magnesian, Wo content of them should be lower than that of anhedral clinopyroxene. There is, however, no systematic difference in Wo content between them. If the ferric content for euhedral clinopyroxene is higher than that of anhedral clinopyroxene, the difference in Mg/Mg+Fe(tot) can be explained. However, the variation of XMg can not be explained by the difference of ferric content in clinopyroxene. According to the method proposed by Lindsley and Anderson(1983), ferric content

of clinopyroxene is calculated(Table4-1). The ferric content corrected $Mg/Mg+Fe^{2+}$ of the euhedral clinopyroxene is still lower than that of anhedral clinopyroxene(Table4-1).

The size dependence of Mg-Fe partitioning between olivine and clinopyroxene is also examined. In Fig.4-9, the size of clinopyroxene and partitioning coefficient are plotted. The distribution coefficient for each clinopyroxene is unity when the size is larger than 1mm.

The difference in distribution coefficient is caused by the size difference of clinopyroxene. The core of the grain larger than 1mm preserves magmatic composition. Otherwise XMg of the core of the grain smaller than 1mm is changed during the cooling and the distribution coefficient is larger than unity.

Clinopyroxene below 1mm is partially reequilibrated with olivine by subsolidus diffusion. Diffusion coefficient of Ca-Mg in clinopyroxene is 10^{-15} cm^2/s at 1200°C(Brady and McCallister, 1983). This is probably comparable to Fe-Mg diffusion(Rietmeijer, 1983). Therefore duration of diffusion is more than 3×10^5 years.

In Unit I, olivine is also homogenized. Diffusion coefficient in Fe-Mg and Ni in olivine is more than 10^{-13} cm^2/s at 1200°C(Morioka, 1981), subsolidus diffusion duration for 1cm olivine is about 3×10^5 years. According to olivine-spinel geospeedmeter(Ozawa, 1984), cooling rate of the Toba ultramafic complex is 10^{-1} to 10^{-3} °C per year. These estimations are consistent with each other.

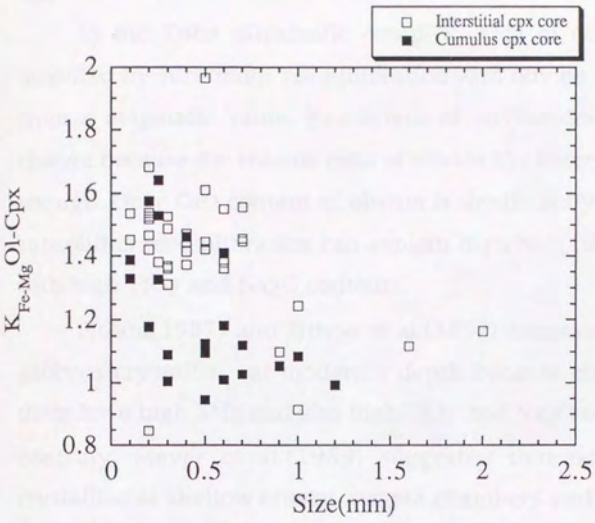

Fig.4-9 Correlation between grain size of clinopyroxene and its Fe-Mg distribution coefficient to olivine in Unit I. The symbols are similar to Fig.4-5.

Implication for oceanic cumulate

In the Toba ultramafic complex, XMg of clinopyroxene is modified by subsolidus reequilibration with olivine and is different from a magmatic value. Fo content of olivine does not strongly change because the volume ratio of olivine to clinopyroxene is large enough. Only CaO content of olivine is significantly modified. This subsolidus reequilibration can explain high XMg of clinopyroxene with high TiO_2 and Na_2O contents.

Elthon(1987) and Elthon et al.(1992) suggested that oceanic gabbros crystallize at moderate depth because clinopyroxene in them have high XMg and also high TiO_2 and Na_2O contents. On the contraly, Meyer et al.(1989) suggested that oceanic gabbros crystallize at shallow crustal magma chambers and high TiO_2 and Na_2O content of clinopyroxene are caused by trapped liquid crystallization. Elthon et al.(1992) discussed the possibility of interstitial liquid crystallization and rejected the idea because interstitial liquid crystallization cannot produce CPXs with anoumalously high XMg(above 0.88). But they did not discuss the possibility of subsolidus reequilibration.

In Fig.4-10, olivine chemical composition in oceanic cumulates is compiled from the data of Elthon(1987) and Meyer et al.(1989). Olivine in oceanic cumulates is characterized by relatively low CaO content(below 0.1wt.%). The Fo content ranges from 88 to 72. Olivine has homogeneous composition in each grain and in one thin section(Meyer et al., 1989).

In Fig.4-11, clinopyroxene chemical composition coexisting with olivine in oceanic cumulates is compiled from the data of Elthon(1987) and Meyer et al.(1989). Clinopyroxene has higher XMg than that of coexisting olivine. CaO content of clinopyroxene

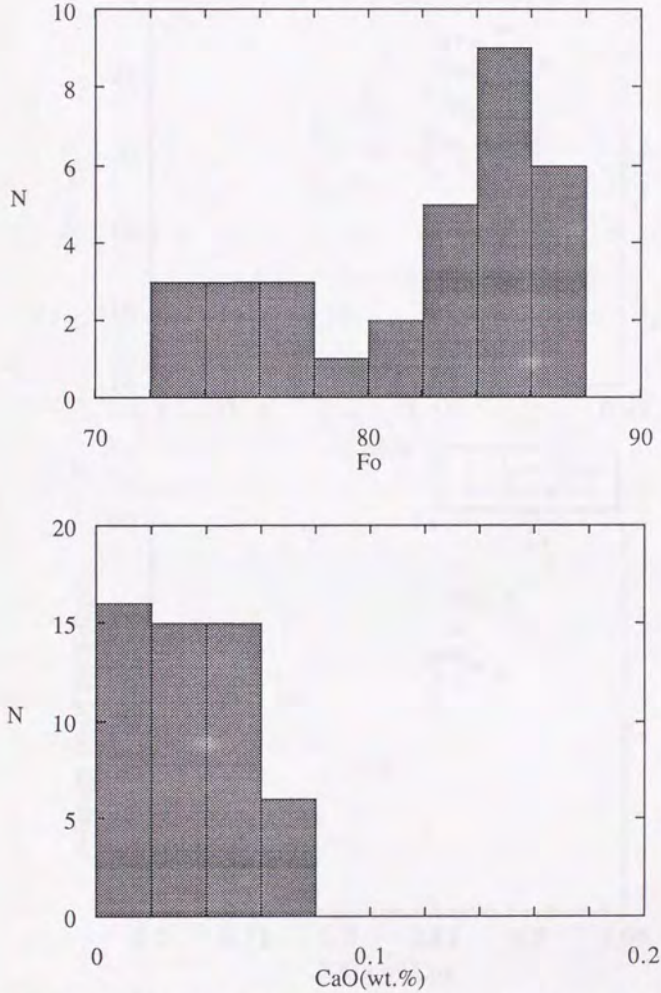

Fig.4-10 Chemical composition of olivine in oceanic cumulates. The data are compiled from Elthon(1987) of Mid-Cayman Rise and Meyer et al.(1989) of Southwest Indian Ridge.

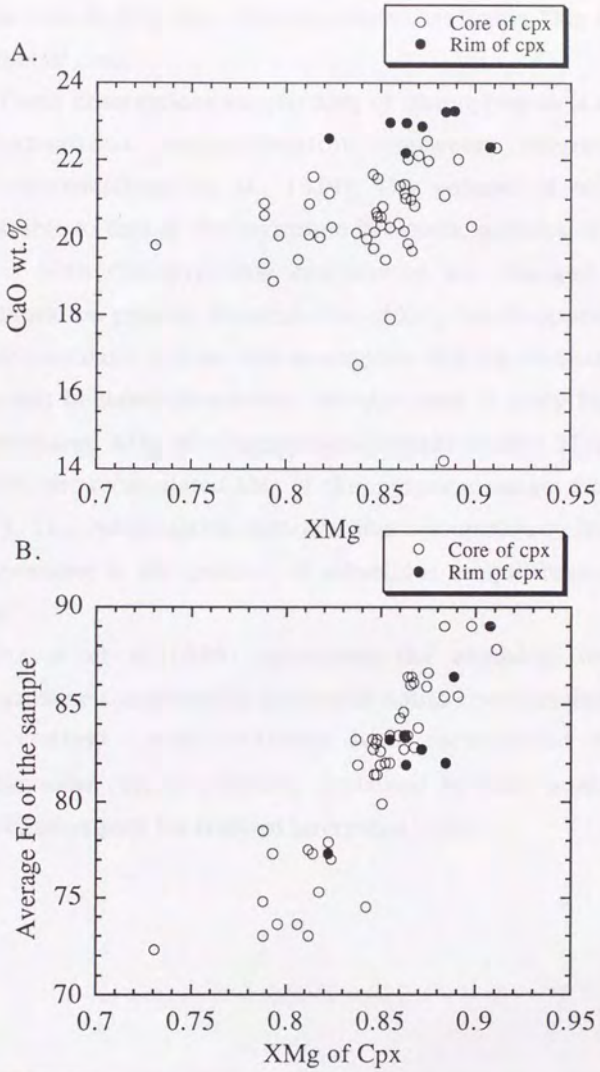

Fig.4-11 A. Chemical composition of clinopyroxene coexisting with olivine of oceanic cumulates: open circle; core of clinopyroxene, filled circle; rim of clinopyroxene. B. Correlation between XMg of clinopyroxene and average Fo content of olivine in the sample of oceanic cumulate: open circle, core of clinopyroxene, filled circle; rim of clinopyroxene. The data source is the same as for Fig.4-10.

correlates to its XMg. Rim of clinopyroxene has higher XMg and CaO than that of core.

These observations suggest XMg of clinopyroxene is affected by subsolidus reequilibration between olivine and clinopyroxene(Obata et al., 1974). The volume of olivine is comparable to that of clinopyroxene in oceanic gabbros, therefore XMg of both clinopyroxene and olivine are changed in the reequilibration process. Recalculation of XMg for clinopyroxene in oceanic cumulates is done with assumption that Mg-Fe distribution coefficient between olivine and clinopyroxene is unity(Fig.4-12). The measured XMg of clinopyroxene ranges from 0.91 to 0.73, however, the recalculated XMg of clinopyroxene ranges from 0.89 to 0.73. This recalculation indicates that anoumalously high XMg clinopyroxene is the product of subsolidus reequilibration with olivine.

Meyer et al.(1989) calculated the chemical trend of clinopyroxene controlled by interstitial liquid crystallization. High TiO_2 content with relatively high recalculated XMg of clinopyroxene can be probably explained by their equilibrium crystallization path for trapped interstitial liquid.

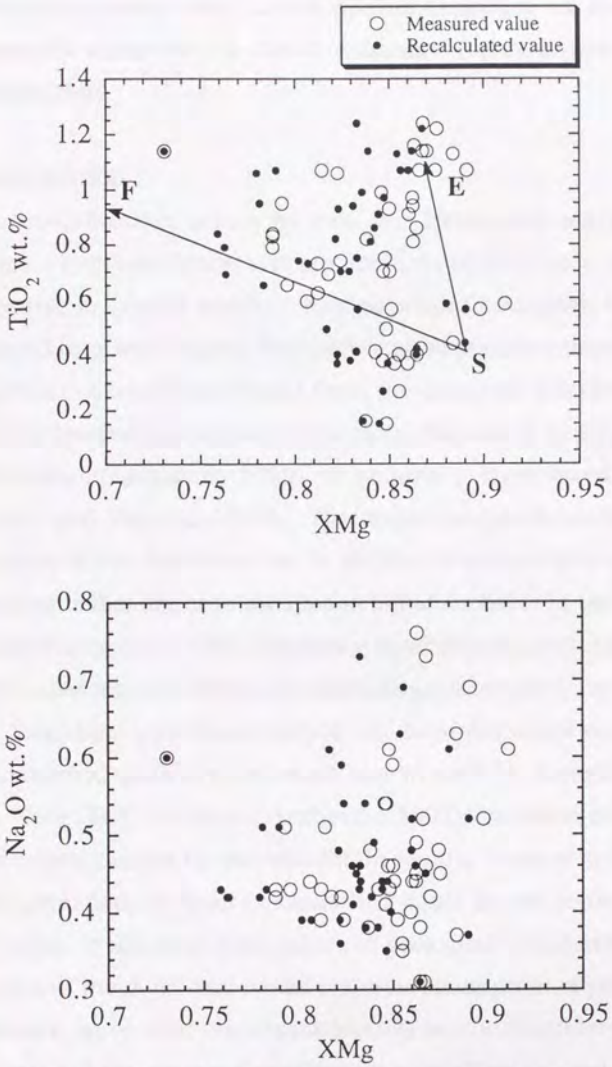

Fig.4-12. Measured(open circle) and recalculated(solid circle) chemical composition of clinopyroxene in oceanic cumulates. Recalculation of XMg of clinopyroxene was done with assumption that initial Mg-Fe distribution coefficient between olivine and clinopyroxene is unity and the system is closed. The data source is the same as for Fig.4-10. Crystallization path of clinopyroxene calculated by Meyer et al.(1989) is also shown. The crystallization path for equilibrium crystallization of interstitial liquid is from S to E and for fractional crystallization is from S to F.